

## Aberystwyth University

### *Elaia, Pergamon's maritime satellite*

Seeliger, Martin; Pint, Anna; Feuser, Stefan; Riedesel, Svenja; Marriner, Nick; Frenzel, Peter; Pirson, Felix; Bolten, Andreas; Brückner, Helmut

*Published in:*

Journal of Quaternary Science

*DOI:*

[10.1002/jqs.3091](https://doi.org/10.1002/jqs.3091)

*Publication date:*

2019

*Citation for published version (APA):*

Seeliger, M., Pint, A., Feuser, S., Riedesel, S., Marriner, N., Frenzel, P., Pirson, F., Bolten, A., & Brückner, H. (2019). Elaia, Pergamon's maritime satellite: the rise and fall of an ancient harbour city shaped by shoreline migration. *Journal of Quaternary Science*, 34(3), 228-244. <https://doi.org/10.1002/jqs.3091>

#### **General rights**

Copyright and moral rights for the publications made accessible in the Aberystwyth Research Portal (the Institutional Repository) are retained by the authors and/or other copyright owners and it is a condition of accessing publications that users recognise and abide by the legal requirements associated with these rights.

- Users may download and print one copy of any publication from the Aberystwyth Research Portal for the purpose of private study or research.
- You may not further distribute the material or use it for any profit-making activity or commercial gain
- You may freely distribute the URL identifying the publication in the Aberystwyth Research Portal

#### **Take down policy**

If you believe that this document breaches copyright please contact us providing details, and we will remove access to the work immediately and investigate your claim.

tel: +44 1970 62 2400  
email: [is@aber.ac.uk](mailto:is@aber.ac.uk)

1 Martin Seeliger<sup>1\*</sup>, Anna Pint<sup>2</sup>, Stefan Feuser<sup>3</sup>, Svenja Riedesel<sup>4</sup>, Nick Marriner<sup>5</sup>, Peter  
2 Frenzel<sup>6</sup>, Felix Pirson<sup>7</sup>, Andreas Bolten<sup>2</sup> & Helmut Brückner<sup>2</sup>

3

4 **Elaia, Pergamon's maritime satellite: the rise and fall of an ancient harbour city shaped**  
5 **by shoreline migration**

6 <sup>1</sup> Department of Physical Geography, Faculty of Geosciences, Goethe-University Frankfurt, Germany

7 <sup>2</sup> Institute of Geography, University of Cologne, Germany

8 <sup>3</sup> Institute of Classical Studies, Kiel University, Germany

9 <sup>4</sup> Department of Geography and Earth Sciences, Aberystwyth University, United Kingdom

10 <sup>5</sup> CNRS, Laboratoire Chrono-Environnement UMR 6249, Université de Bourgogne-Franche-Comté, France

11 <sup>6</sup> Institute of Earth Sciences, Friedrich-Schiller University Jena, Germany

12 <sup>7</sup> German Archaeological Institute (DAI), Istanbul, Turkey

13

14 \*Corresponding author: seeliger@em.uni-frankfurt.de (Martin Seeliger)

15

16 **Running title: Shoreline Migration Elaia**

17 **Keywords: Palaeogeography, coastal evolution, Micropalaeontology, Aegean, Sea-level**  
18 **fluctuations**

19

20 **Abstract**

21 Throughout human history, communication and trade were key to societies. Because maritime  
22 trade facilitates the rapid transportation of passengers and freight at relatively low costs,  
23 harbours became hubs for traffic, trade, and exchange. This general statement holds true for  
24 the Pergamenian kingdom, which ruled wide parts of today's western Turkey during  
25 Hellenistic times. Its harbour, located at the city of Elaia on the eastern Aegean shore, was  
26 used extensively for commercial and military purposes.

27 This study reconstructs the coastal evolution in and around the ancient harbour of Elaia and  
28 compares and contrasts the observed environmental modifications with archaeological and  
29 historical findings. We used micropalaeontological, sedimentological, and geochemical  
30 proxies to reconstruct the palaeoenvironmental dynamics and evolution of the ancient  
31 harbour. The geoarchaeological results confirm the archaeological and historical evidence of  
32 Elaia's prime during Hellenistic and early Roman times, and the city's gradual decline during  
33 the late Roman period. Furthermore, our study demonstrates that Elaia holds a unique position  
34 as a harbour city during ancient times in the eastern Aegean region, because it was not  
35 completely influenced by the high sediment supply associated with river deltas. Consequently,  
36 no dredging of the harbour basins is documented, creating exceptional geo-bio-archives for  
37 palaeoenvironmental reconstructions.

38

## 39 **Introduction**

40 Around the end of the Holocene marine transgression, circa 6000 BP (Lambeck, 1996;  
41 Lambeck and Purcell, 2007), sea-level stabilisation enabled ancient societies to settle along  
42 Mediterranean shores (Anthony *et al.*, 2014; Murray-Wallace and Woodroffe, 2014; Vacchi  
43 *et al.*, 2014, 2016a; Khan *et al.*, 2015; Benjamin *et al.*, 2017; Seeliger *et al.*, 2017). For many  
44 civilisations, a connection to the sea was an important factor in establishing a flourishing  
45 settlement. In the Aegean, this statement is, for example, supported by the Neolithic  
46 settlements of Hoca Çeşme in Thrace (Başaran, 2010; Özbek, 2010), Hamaylıtarla on the  
47 Gallipoli peninsula (Özbek, 2010) and Çukuriçi Höyük near ancient Ephesus (Horejs, 2012;  
48 Horejs *et al.*, 2015; Stock *et al.*, 2015). All of them were situated less than 4 km from the sea,  
49 much closer than they are today (Ammerman *et al.*, 2008). There are many examples from the  
50 Aegean that demonstrate that the fate of ancient settlements was closely linked to migrating  
51 shorelines and changing sea level. In Western Anatolia, Troy, Miletos, Ainos, Ephesus, and  
52 Liman Tepe are the most prominent ones. Their rise and fall as harbour cities were shaped  
53 essentially by environmental changes, which have been described by many geoarchaeological  
54 studies (Kraft *et al.*, 1977, 2007; Kayan, 1999, 2014; Brückner *et al.*, 2006, 2013, 2015;  
55 Goodman *et al.*, 2008, 2009; Delile *et al.*, 2015; Shumilovskikh *et al.*, 2016; Seeliger *et al.*,  
56 2018).

57 Here, we investigate the evolution of the coastal configuration around the city of Elaia that  
58 hosted the former military and commercial harbour of ancient Pergamon in Hellenistic and  
59 Roman times. Since 2013, several papers have focused on the environmental evolution of the  
60 Bay of Elaia. By analysing sediment cores taken inside and outside the main harbour basin of  
61 Elaia, the closed harbour, Seeliger *et al.* (2013) demonstrated how it was built in the first half  
62 of the 3<sup>rd</sup> century BC, how it has been used during the apogee of Elaia, and why it was  
63 abandoned due to massive sedimentation in late Roman times (Fig. 2). Seeliger *et al.* (2014)  
64 used optically stimulated luminescence (OSL) dating and electrical resistivity tomography  
65 (ERT) measurements to probe the construction style and age of presently submerged walls  
66 circa 1–2 km south of the city and interpret these structures as the remains of saltworks  
67 constructed using spolia in Late Antiquity, a time when the harbours of Elaia were no longer  
68 navigable and the people had abandoned the city (Fig. 2a). Pint *et al.* (2015) performed  
69 detailed analyses of foraminifera and ostracoda, in combination with 3D-ERT measurements,  
70 to detect the style and usability of presumed Hellenistic ship sheds in the open harbour area of  
71 Elaia. They concluded that the open harbour and its ship sheds were operational during  
72 Hellenistic times, but were no longer navigable from Roman Imperial times onwards.

73 Furthermore, Shumilovskikh *et al.* (2016) undertook a palynological investigation of sediment  
74 core Ela 70, taken from inside the closed harbour basin. This work precisely reconstructed the  
75 palaeoenvironmental conditions and the vegetation history of the Bay of Elaia during the last  
76 7500 a. Finally, Seeliger *et al.* (2017) described a new sea-level indicator based on  
77 foraminifera associations in the context of the transgressive contact. Based on these data, they  
78 reconstruct a relative sea-level (RSL) history for the area showing steadily rising sea-level  
79 since 7500 BP and today's sea-level maximum. By comparing and contrasting their RSL  
80 history to curves from nearby Greek sites in the Aegean they reviewed the RSL evolution of  
81 the Aegean since the mid-Holocene. Furthermore, Feuser *et al.* (2018) recently published a  
82 summary presenting the state-of-the-art knowledge on the use of the Elaia's harbours, from an  
83 archaeological perspective.

84 In this article, we aim to integrate key findings of previous studies with new  
85 chronostratigraphic results to (i) investigate the causes of environmental modifications; (ii) to  
86 reconstruct the changes in the shoreline of the Bay of Elaia; and (iii) to provide fresh insights  
87 into the link between shoreline changes and human-environment interactions during Elaia's  
88 settlement period. Therefore, we focus on the time period from 1500 BC onwards, which  
89 covers Elaia's prime as Pergamon's prospering harbour. In addition, we compare our results  
90 with other ancient coastal settlements in Asia Minor to furnish a broader view on different  
91 environmental changes, which shaped the rise and fall of ancient coastal settlements in the  
92 eastern Aegean.

93

#### 94 **Physical setting**

95 Elaia is located in the north-western part of modern Turkey (Figs. 1a, b). The study area is  
96 part of the westwards drifting Aegean-Anatolian microplate (Vacchi *et al.*, 2014). As a  
97 consequence of this drift, several E-W oriented rift structures were formed in the late  
98 Miocene, such as the Bergama graben, and its tributary, the Zeytindağ graben. This tectonic  
99 ensemble represents a fractured zone, which was favourable to the evolution of the Kaikos  
100 valley (Vita-Finzi, 1969; Aksu *et al.*, 1987; Seeliger *et al.*, 2013; Fig. 1a). The Karadağ  
101 Mountains to the west and the Yuntdağ Mountains to the east border the Gulf of Elaia (Figs.  
102 1, 2). The wide alluvial plain and the cusate delta of the Bakır Çay (ancient name: Kaikos)  
103 are located to the west of the Bay of Elaia, separated by the flat ridge of Bozyertepe (40 m  
104 a.s.l. (above present sea level; Fig. 2)).

105 The Elaia coastal zone has a typical Mediterranean climate, Csa according to Koeppen and  
106 Geiger's nomenclature, with hot and dry summers, and mild and humid winters (Yoo and

107 Rohli, 2016). Therefore, heavy rain and torrential rivers are major morphological agents  
108 (Brückner, 1994; Jeckelmann, 1996). Our own observations confirmed that the sea in the Bay  
109 of Elaia turns brownish due to excessive wash-down of colluvial material during heavy rain.  
110 Due to the steepness of the Yuntdağ Mountains, this effect is even stronger in the eastern part  
111 of the Bay of Elaia (Fig. 2c).

112

### 113 **Historical background**

114 Pergamon is one of the most famous ancient settlements in Turkey, frequently mentioned with  
115 Troy, Miletos, Ainos, and Ephesus (Kraft *et al.*, 1980, 2003, 2007; Kayan, 1999; Brückner *et*  
116 *al.*, 2013; Seeliger *et al.*, 2018). Thanks to shifts in the settlement areas, its impressive  
117 monumental structures, its important library and school of philosophers, Pergamon provides  
118 detailed insights into the urban structure of a Hellenistic city (Radt, 2016). Soon after  
119 Alexander the Great died in Babylon in 323 BC, the so-called “Wars of the Diadochi”  
120 affected great tracts of his empire (Cartledge, 2004). In a later stage of these fights, the  
121 dynasty of the *Attalids* came to power in the Kaikos region and established – in alliance with  
122 Rome – a powerful kingdom in Asia Minor, which, during its prime under King Eumenes II  
123 (197–159 BC) ruled the western half of present-day Turkey. In 133 BC, their realm was  
124 integrated into the growing Roman Empire (Hansen, 1971; Pirson and Scholl, 2015; Radt,  
125 2016; Fig. 1c). Pergamon’s location on top of the 330 m high Acropolis hill, overlooking the  
126 surrounding Kaikos plain, was excellent for security and defence, but complicated trade and  
127 transport. Furthermore, the Pergamenians were in need of a maritime harbour. They found it  
128 in the nearby city of Elaia, located on the Aegean Sea approximately 26 km south-west of  
129 Pergamon (Figs. 1a, 2a). According to current research knowledge, Elaia came under  
130 Pergamenian hegemony during the regency of Eumenes I (263–241 BC; Pirson, 2004; Radt,  
131 2016). Additionally, *Strabo* mentioned Elaia as the commercial harbour of the Pergamenians  
132 and as the military base of the *Attalids* (*Geographica XIII, 1, 67; XIII, 3, 5*). Further evidence  
133 from literary sources and archaeological findings emphasises the close link between Elaia and  
134 Pergamon (Pirson, 2004, 2008, 2010, 2011, 2014). The harbour zone of Elaia was divided  
135 into three parts (Fig. 2).

136 First, the closed harbour basin (I in Fig. 2) within the fortification walls, which was built in  
137 early Hellenistic times. It was protected from the sea and enemies by two massive  
138 breakwaters; nowadays they are landlocked, but still visible. Geoarchaeological research has  
139 revealed that substantial siltation occurred between the 3<sup>rd</sup> and the end of the 4<sup>th</sup> centuries AD;  
140 from the 5<sup>th</sup> century AD onwards the closed harbour was no longer navigable (Pirson, 2007,

141 2008; Seeliger *et al.*, 2013, 2017). Second, a circa 250 m long open harbour zone (II in Fig. 2)  
142 stretching from the southern breakwater of the closed harbour south-eastwards to the point  
143 where an internal wall reached the waterfront. This so-called *diateichisma* divided the city  
144 area into a northern, densely-populated part and a southern one (Pirson, 2011; Pint *et al.*,  
145 2015). Third, a beach harbour extended from south of the diateichisma to the south-eastern tip  
146 of the city wall (III in Fig. 2). This area was probably used as a multifunctional military zone,  
147 including dockyards where warships were beached and maintenance work was conducted  
148 (Pirson, 2011, 2014; Pint *et al.*, 2015).

149 Palaeogeographical research was conducted to assess small-scale palaeoenvironmental  
150 changes in the Bay of Elaia. Because Elaia served as the satellite harbour city of Pergamon  
151 during its prime, previous research focussed on the function and temporal use of the different  
152 harbours identified (Seeliger *et al.* 2013, 2017; Pint *et al.* 2015). Although detailed research  
153 was conducted, some key questions remain. Key knowledge gaps include: (i) How did coastal  
154 and RSL changes influence the human occupation history of the city? (ii) To what extent does  
155 Elaia fit with the traditional “rise and fall model” linked to shoreline migration?

156 Seeliger *et al.* (2017) took a first step toward answering these questions, by publishing a RSL  
157 curve for Elaia and comparing it to the RSL histories of other study areas in the Aegean. Here  
158 we seek to further explore the role of Elaia as an example of shoreline migration and human  
159 settlement changes in the Aegean during ancient times. This research is based on 19 sediment  
160 cores, drilled along five transects perpendicular to the present shoreline (Fig. 2a). This  
161 approach has been widely adopted in Mediterranean coastal studies (e.g. Kraft *et al.*, 2007;  
162 Goodman *et al.*, 2008, 2009; Kayan, 2014; Marriner *et al.*, 2014; Delile *et al.*, 2015,  
163 Morhange *et al.*, 2016; Evelpidou *et al.*, 2017; Flaux *et al.*, 2017; Giaime *et al.*, 2017;  
164 Pennington *et al.*, 2017; Seeliger *et al.*, 2018) to investigate lateral and vertical changes in the  
165 sediment stratigraphy and to probe the evolution of the landscape, notably shoreline  
166 migration.

167

## 168 **Material and methods**

### 169 *Geoarchaeological fieldwork*

170 Sediment cores were extracted using an Atlas Copco Cobra TT vibracorer with open steel  
171 auger heads (diameter: 6 and 5 cm, respectively) in the surroundings of the Bay of Elaia,  
172 down to a maximum depth of 12 m b.s. (below the surface). On-site, sediments were  
173 described according to grain size and colour (Ad-hoc-AG Boden, 2005; Munsell Soil Color  
174 Charts) and bulk samples for laboratory analyses were taken from the open sediment cores

175 (5–6 samples/metre). All coring sites were georeferenced using a Leica DGPS System 530  
176 (accuracy of  $\leq 2$  cm in all three dimensions; Seeliger *et al.*, 2013, 2014); they are reported in  
177 m above sea level (a.s.l.) and m below the surface (b.s.).

178

### 179 *Sedimentology and geochemistry*

180 Multi-proxy laboratory analyses were conducted (Ernst, 1970; Hadler *et al.*, 2013; Bartz *et*  
181 *al.*, 2015, 2017; Seeliger *et al.*, 2013, 2018). Samples were air-dried and sieved to separate the  
182  $\leq 2$  mm grain-size fraction for further analyses. For laser-based grain-size analysis  
183 (Beckman Coulter LS13320), the organic content was decomposed using 15 % hydrogen  
184 peroxide (H<sub>2</sub>O<sub>2</sub>). Afterwards, sodium pyrophosphate (Na<sub>4</sub>P<sub>2</sub>O<sub>7</sub>; concentration: 47 g/l) was  
185 taken as a dispersant. Each sample was measured three times in 116 classes, determining  
186 grain-size distributions in a range from 0.04 to 2000  $\mu$ m. For the calculation of grain-size  
187 parameters (Folk and Ward, 1957), we used the software package GRADISTAT (Blott and  
188 Pye, 2001). To estimate the organic content, measurements of LOI (loss on ignition) were  
189 performed by oven drying (105 °C for 12 h to determine the water content) and combustion in  
190 a furnace (550 °C for 4 h to determine the organic substance). Electric conductivity was  
191 measured in an aqueous solution (5 g sediment in 25 ml deionised water) with a glass  
192 electrode connected to a Mettler Toledo InLab®731-2m instrument. To determine different  
193 sedimentary units, characteristic elements (e.g. Fe, K, Ca, Ti, etc.) were measured using a  
194 portable XRF (X-ray fluorescence) spectrometer (Niton XI3t 900 GOLDD; Vött *et al.*, 2011;  
195 Lubos *et al.*, 2016). To ensure comparability with all XRF analyses and to reduce grain-size  
196 dependency, each sample was ground to powder in a ball triturator (Retsch PM 4001) and  
197 then pressed into pills.

198

### 199 *Micropalaeontology*

200 For microfaunal analysis, selected 1 cm<sup>3</sup> samples were wet-sieved using a 100  $\mu$ m mesh.  
201 Under a stereoscopic microscope, at least 300 ostracod valves and foraminifer tests,  
202 respectively, were picked from appropriate splits of the residues of every sample. If less than  
203 300 specimens were present within a sample all were picked. Species were identified and  
204 counted according to Bonaduce *et al.* (1975) and Joachim and Langer (2008) for ostracods as  
205 well as Cimermann and Langer (1991), Meriç *et al.* (2004), and Murray (2006) for  
206 foraminifers.

207

### 208 *Chronology*

209 The chronological framework is based on  $^{14}\text{C}$ -AMS age determinations. Depending on the  
210  $\delta^{13}\text{C}$ -value, each sample was calibrated using either the IntCal13 or the MARINE13  
211 calibration curve in Calib 7.1 (Reimer *et al.*, 2013) with a marine reservoir age of  $390\pm 85$  a  
212 and a  $\Delta R$  of  $35\pm 70$  a (Siani *et al.*, 2000). Siani *et al.*, (2000) used shells of known age  
213 sampled in the Dardanelle Strait and stored in the Muséum National d'Histoire Naturelle,  
214 Paris to calculate the local marine reservoir age and its  $\Delta R$ . As there are no further studies in  
215 the closer vicinity of Elaia, this value has been chosen to correct the calibrations on marine  
216 material. Finally, because the spatio-temporal variation of the marine reservoir effect for the  
217 Aegean is still not completely understood, the  $^{14}\text{C}$ -ages of marine carbonates should be  
218 interpreted carefully. Because this paper presents archaeological-related data, all ages are  
219 presented in cal a BC/AD. Tab. 1 provides all mentioned ages in cal a BP.

220

## 221 **Results of Ela 57 and Ela 12**

222 The coring profiles of the Elaia region, a selection of 19 is presented here (Fig. 2a), can be  
223 divided into two groups: those, which reach bedrock and those that do not. Additionally, the  
224 sedimentation pattern in the western part of the Bay (transects A–A' and B–B') differs  
225 significantly from that of the eastern part (D–D', E–E', and F–F'). This is demonstrated by  
226 the detailed description of two cores, one from each group: Ela 57 (Figs. 3, 4) and Ela 12  
227 (Figs. 5, 6). Additionally, Ela 58 (Pint *et al.*, 2015) is considered in order to present all  
228 sedimentary units (Fig. 2a). A detailed description of the profiles Ela 57 and Ela 12 is stated  
229 in Appendix 1.

230

## 231 **Interpretation**

### 232 Introduction of sedimentary units

233 Many sediment cores from the Elaia area are summarised by the classification in units of  
234 typical environmental characteristics. Their definition based on geochemical, granulometric,  
235 and micro-faunistic parameters of cores Ela 57 and 12. This compilation is intended to shorten  
236 the interpretation of the cores (Fig. 7) and described in detail in Appendix 2.

237

### 238 Sediment core-based reconstruction of palaeoenvironments

239 Based on the previous sections, coring profiles Ela 57 and Ela 12 are interpreted as follows:

240

241 *Sediment core Ela 57 representing the eastern part of the Bay of Elaia*



242 The palaeogeographical evolution of the eastern part of the Bay of Elaia is exemplified by  
243 Ela 57 (Figs. 2, 3, 4).

244 Neogene bedrock (unit 1), encountered at 5.42 m b.s., forms the base of numerous cores in the  
245 study area. The calcareous sandstone, outcropping nearby, was used to construct the harbour  
246 breakwaters (Seeliger *et al.*, 2013, 2014). The overlying unit 2 represents the transgressive  
247 littoral unit during the Holocene sea-level rise. The high-energy environment is obvious from  
248 a number of gravels, the coarse grain size, and patches of seagrass. The low biodiversity and  
249 the sole occurrence of robust foraminifers in the lower part of unit 2, such as *Ammonia*  
250 *compacta* and *Elphidium crispum*, are evidence for the high-stress level of this littoral  
251 environment in which only a few species are able to survive (Seeliger *et al.*, 2017). The  
252 fining-upward sequence is due to increasing water depth, which is also reflected by a higher  
253 biodiversity. The Holocene transgression reached this area at the end of the 3<sup>rd</sup> millennium BC  
254 (2198–2035 cal a BC), which is far before the human occupation phase of Elaia. The second  
255 age of Ela 57 dates to late Hellenistic/ early Roman times (165 cal a BC–1 cal a BC/AD), the  
256 period when Elaia flourished. Rising sea level led to the formation of a shallow water body  
257 represented by unit 4. It shows a fining-upward sequence due to the inland migration of the  
258 shoreline, leading to reduced wave action. This results in a lower amount of shell debris and  
259 the occurrence of preserved valves. The microfaunal association indicates a shallow marine  
260 environment. Based on our results from inside the closed and open harbours, relative sea level  
261 at the turn of the eras was approximately 1.50 m lower than today. Thus, water depth at this  
262 time should not have exceeded more than 1.30–1.50 m (Pint *et al.*, 2015; Seeliger *et al.*,  
263 2017).

264 By then, the surroundings of this part of the city area may have served as a beach harbour area  
265 where foreign soldiers landed and repaired their ships and put up camp, thus staying outside  
266 the actual city area. This custom was normal for small to medium-sized cities at this time,  
267 because it offered a higher level of security for the inhabitants. As the nearby coring Ela 56  
268 does not show any marine or littoral sediments, the site of Ela 57 always lay in a nearshore  
269 position, close to the landing area for ships and smaller vessels. A sharp contact at -1.61 m  
270 a.s.l. suggests a sudden end to this sheltered marine water body, possibly due to a massive  
271 deposition engendered by torrential floods, triggered by heavy rainfall. Such erosional events  
272 were favoured by the widespread deforestation of this area during Hellenistic and Roman  
273 times (Shumilovskikh *et al.*, 2016). The erosional contact at the base, the fining-upward  
274 sequence, the fluvial character of the stratum including brick fragments, seeds, charcoal, and  
275 even bones, all washed down from the nearby slopes, as well as the absence of microfauna,

276 support this interpretation. The upper part of this unit dates to Roman Imperial times. Since  
277 the dated olive stone (Ela 57/8H; Tab. 1) is very robust and may have been reworked, the age  
278 should only be regarded as a minimum age. It seems that the fluvial deposition most probably  
279 occurred during the final phase of the settlement of Elaia in late Roman times which may  
280 have influenced the final decision to abandon the city. Since the area around coring site Ela 57  
281 suddenly became terrestrial, the second transition of the shoreline, often indicated by a second  
282 littoral phase (unit 5), is missing. That the area was at least partly influenced by human impact  
283 is evidenced by the anthropogenically-disturbed colluvium (unit 7b), which forms the top  
284 layer.

285

#### 286 *Sediment core Ela 12 representing the western part of the Bay of Elaia*

287 The palaeogeographical evolution of the western Bay of Elaia is exemplified by profile Ela 12  
288 (Figs. 2, 5, 6).

289 At the bottom, the profile shows sediments of a sheltered embayment (unit 4) where  
290 *Posidonia oceanica* meadows could thrive on the sea floor (Vacchi *et al.*, 2016b). Well-  
291 preserved marine bivalves support this idea. The geochemical data and the microfaunal  
292 association indicate a near-shore environment as typically open marine species are missing  
293 (Pint *et al.*, 2015). A radiocarbon age of 803–568 cal a BC dates this part to the first half of  
294 the 1<sup>st</sup> millennium (Geometric-Archaic times). Very little is known about the history of the  
295 study area during this period (Pirson and Scholl, 2015; Fig. 1c). The shallow marine  
296 environment prevailed for some time until sediments from the nearby Bozyertepe were  
297 increasingly washed into the embayment. This caused a regression of the shoreline with  
298 decreasing water depth, and the establishment of littoral unit 5, which is of progradational  
299 origin. Compared to the transgressive unit 2 of Ela 57, the progradational unit 5 of Ela 12 has  
300 a similar microfaunal composition but displays a coarsening-upward sequence. The  
301 environmental stress led to low biodiversity, while the increased occurrence of mollusc and  
302 shell debris provides evidence of intense wave energy. It can be excluded that the advancing  
303 delta of the Kaikos (Bakır Çay) played a major role in the silting up of this inner part of the  
304 Bay of Elaia because neither Ela 12 nor the whole transects A–A' and B–B' contains fluvial-  
305 deltaic sediments and the Bozyertepe acts as a barrier for this material (Fig. 2a). The littoral  
306 unit ends at -2.78 m a.s.l., when terrestrial processes become dominant. This is the onset of  
307 the accumulation of colluvium (unit 7a). Since transect A–A' is situated at a distance from the  
308 settled area of Elaia, it is not surprising that no direct indicators of human impact are found  
309 inside the colluvium.

310

311 *Landscape evolution based on coring transects*

312 After the detailed description of two representative sediment cores, five transects and one  
313 single coring are discussed to clarify the landscape evolution of the Bay of Elaia (Fig. 8).

314 Transect A–A' consists of three different types of profiles. The coastal corings Ela 11 and 12  
315 show a typical regressive sedimentary sequence (Fig. 8). Increased sedimentation in the  
316 context of the settlement period of Elaia led to the silting up of a low energy, shallow marine  
317 water body (unit 4), which turned to a littoral progradation unit 5 and later to a natural  
318 colluvial environment (unit 7a). Ela 14 and 20 reach the bedrock, which is topped by  
319 nearshore littoral deposits (unit 2); these are overlain by natural colluvium. The rising bedrock  
320 towards the Bozyertepe causes the landward thinning of the littoral strata. Since core Ela 19  
321 does not contain marine, fluvial, or littoral units, the maximum marine transgression in A–A'  
322 is close to coring Ela 20, where it is dated to the end of the 2<sup>nd</sup> millennium BC. Transect B–  
323 B' represents the marine transgression into the valley between the Acropolis to the east and the  
324 Bozyertepe to the west (Fig. 8). It provides results comparable to A–A'. Coastal corings Ela 1  
325 and 2 demonstrate a regressive sediment sequence, similar to Ela 11 and 12. They represented  
326 a shallow water body in this area of the Bay of Elaia at least since the first half of the 1<sup>st</sup>  
327 millennium BC. According to these results, the areas of Ela 1 and 2 were still under marine  
328 influence during the main occupation phase of Elaia (Figs. 1c, 2). Since Ela 9 only shows  
329 colluvial sediments, coring Ela 3/17 marks the maximum marine transgression of B–B'. This  
330 dates to the end of the 3<sup>rd</sup> millennium BC. Ela 58 ("C") is the only core in this area, which  
331 includes a shallow marine unit (unit 3) with high biodiversity. It dates to the 4<sup>th</sup>/5<sup>th</sup> millennia  
332 BC. As in the eastern transects, massive fluvial input ended the shallow marine conditions and  
333 initiated a sheltered water area (unit 4), which prevailed throughout Elaia's prime. Later, the  
334 Elaitians dumped material in this area to consolidate the terrain. Transects D–D', E–E', and  
335 F–F' show similar results, and are therefore presented together. The nearshore coring profiles  
336 (Ela 59, 55, and 62) reach the bedrock. The transgressive littoral unit 2, starting with an  
337 erosional disconformity, is covered by unit 4 of a stagnant marine water body. Obviously, the  
338 very low-energy wave conditions prevailed because a progradational unit 5 is missing; all of  
339 the profiles show a smooth transition to colluvial deposits (unit 7a). The inland corings  
340 (Ela 60, 56, and 64) reveal a terrestrial sedimentation pattern interrupted by a layer of fluvial  
341 sediments, most probably caused by torrential floods. The central corings (Ela 61, 57, and 63)  
342 contain key information about the marine extension in this area. All of them display a typical  
343 stratigraphy: the bedrock is overlain by transgressive littoral deposits; then units of a low-

344 energy marine embayment follow and provide evidence of the rising sea level. The shallow  
345 marine deposit is covered by massive input of fluvial sediments, which are topped by human-  
346 induced colluvium. Severe flooding can only be traced in the sediment sequence of the central  
347 and inland corings (Seeliger *et al.*, 2017).

348

### 349 Synopsis

350 With regard to the height above sea level in F–F', a similar age for the maximum marine  
351 ingression in each transect of circa 1500 BC is assumed. Derived from the thickness of the  
352 marine strata of Ela 58 ("C"), the maximum transgressive shoreline is probably located  
353 further inland, i.e. in the area of the later city (where coring was impossible). Ela 61 indirectly  
354 proves this assumption. This is comparable to other ancient cities such as Miletos, Ainos, and,  
355 Ephesus where parts of the cities were also erected on former marine sediments (Brückner *et*  
356 *al.*, 2006, 2015; Kraft *et al.*, 2007; Seeliger *et al.*, 2018). The eastern city district transects and  
357 Ela 58 ("C") show thick sheet-wash deposits which caused massive siltation of the area. In the  
358 case of Ela 58, this could have taken place at the beginning of the 1<sup>st</sup> millennium BC. This is  
359 in good accordance with transect D–D' where this event occurred at a similar date (Ela 61/16;  
360 1149–791 cal a BC). In Ela 57 (E–E'), it is visible just around the turn of the eras, whereas in  
361 Ela 63 (F–F') it occurred in Classical or even Hellenistic times (shortly after Ela 63/10/H;  
362 797–551 cal a BC). However, severe flood events did not occur in the western part of the  
363 embayment (transects A–A' and B–B'). In sum, torrential floods associated with sheet-wash  
364 dynamics occur before and during the intense human settlement activity; they affected the  
365 eastern area of ancient Elaia (Fig. 2). This is, on the one hand, a result of the topography of  
366 the nearby foothills of the steep Yuntdağ Mountains, as compared to the flat Bozyertepe and  
367 the Acropolis (A–A' and B–B'; Fig. 2). On the other hand, the human influence in the eastern  
368 area of the embayment was more intense, leading to degradation of the vegetation cover, soil  
369 degradation, and erosion. At the end of the 1<sup>st</sup> century BC and the beginning of the 1<sup>st</sup> century  
370 AD the settlement pattern of the surroundings of Elaia changed when several of the  
371 Hellenistic farmsteads were abandoned – maybe because of intense floods (Pirson, 2011).

372

### 373 Scenarios of shoreline changes

374 Based on these results, we reconstructed the palaeogeography of the Bay of Elaia for three  
375 different time periods (1500 BC, 300 BC, and AD 500; Figs. 2, 9).

376 **1500 BC:** This is the time of the maximum marine extension in the Bay of Elaia, when sea  
377 level was 3.3–2.4 m lower than today (Seeliger *et al.*, 2017). The coastal zone reached

378 northwards along the slopes of Bozyertepe, almost up to Ela 9 where one of Elaia's  
379 cemeteries was located (Pirson, 2010). This supports the idea that the sea never transgressed  
380 this area during the Holocene. During the maximum marine extension, the later Acropolis of  
381 Elaia protruded into the bay as a peninsula. Nonetheless, it was most probably uninhabited at  
382 this time. The small embayment to the north of Ela 58 may have acted as a preferred landing  
383 area, but as yet this assumption has not been verified by archaeological finds. The same holds  
384 true for the western flank of the Acropolis. In the eastern city area, the shoreline lay close to  
385 the foothills of the Yuntdağ. The former shallow marine and littoral areas of the later city are  
386 easy to identify. Once these had been silted up, and probably also partly filled in by the  
387 inhabitants, they evolved into settled ground after circa 500 BC (Figs. 2, 9).

388 **300 BC:** This scenario represents the period when Elaia started to prosper, when sea level was  
389 just 1.6–2.0 m lower than today (Seeliger *et al.*, 2017). Archaeological findings document  
390 intense human activities on the Acropolis and in the eastern city district (Pirson, 2010). In  
391 addition, palynological data show that various crops were intensively cultivated in the  
392 surroundings of Elaia (Shumilovskikh *et al.*, 2016).

393 Increased sediment load due to soil erosion from Bozyertepe and minor activities of a  
394 nameless ephemeral creek between Bozyertepe and Acropolis caused a shoreline regression in  
395 the western part. None of the corings of A–A' and B–B' show fluvial sediments of the nearby  
396 Kaikos delta. Therefore, its influence concerning the siltation of the inner part of the Bay of  
397 Elaia can be neglected. Wide areas between the Acropolis and Bozyertepe remained marine.  
398 Due to the ongoing seaward shift of the shoreline, a harbour on the western flank of the  
399 Acropolis hill is unlikely at this time. Immediately south of the Acropolis, two harbours were  
400 constructed: the local geomorphology was consolidated and transformed into a closed harbour  
401 basin by the erection of two breakwaters (Seeliger *et al.*, 2013). The water depth of the closed  
402 harbour basin was circa 2.5 m; sufficient for all common battle and merchant ship classes  
403 used by the Pergamenians at that time (Seeliger *et al.*, 2017). Similar considerations also hold  
404 true for the area of the open harbour, including the presumed Hellenistic ship sheds where the  
405 water depth was circa 1.2 m (Pirson, 2010; Pint *et al.*, 2015; Seeliger *et al.*, 2017). As this  
406 area was essentially used to haul vessels into the ship sheds, the water was deep enough to  
407 operate ship sheds. In sum, both harbours were fully accessible and used for military and  
408 commercial purposes at this time (Pirson, 2004; Seeliger *et al.*, 2017; Pint *et al.*, 2015).

409 The eastern city district experienced a regression of the shoreline caused by denudation  
410 processes and human impacts (Shumilovskikh *et al.*, 2016). The coastal area was ideal for  
411 landing battleships while goods were most probably processed in the closed and the open

412 harbours (Pirson 2011, 2014; Seeliger *et al.*, 2017). Torrential floods could have been a  
413 common temporary nuisance in the area, but nothing is known about this from the literature.  
414 Further south the shoreline leaves a narrow passage between the slopes of the Yuntdağ and  
415 the sea (Figs. 1, 2, 9). This underlines Elaia's strategic position: the city did not only serve as  
416 the main harbour of Pergamon, it was also a defensive stronghold, which secured the southern  
417 entrance to the inner realm of the lower Kaikos area (Seeliger *et al.*, 2013; Pirson, 2014; Figs.  
418 1, 2). This topographic setting is comparable to that of Thermopylae in central Greece, where,  
419 in 480 BC, the legendary 300 Spartans fought bravely to withstand the far larger Persian army  
420 due to their strategic use of the landscape (Kraft *et al.*, 1987). Furthermore, it is reasonable to  
421 assume that a defence turret fortified the southern end of the city wall (Pirson, 2010). A turret  
422 would have necessitated a solid foundation when being constructed in a nearshore position;  
423 however, nothing of that kind was detected by coring. In Ela 65 (Figs. 2a, 9) only littoral  
424 sediments dating to the late Hellenistic to Roman periods were revealed.

425 **AD 500:** This scenario represents the time when Elaia was at or near the end of its prime. In  
426 several areas, the shoreline was close to its present position and sea level was only 0.4–0.6 m  
427 lower than today (Seeliger *et al.*, 2017). All corings present terrestrial sedimentation patterns  
428 for this period. The closed harbour basin had been abandoned and nearly silted up. The area  
429 of the former ship sheds was not accessible anymore (Seeliger *et al.*, 2013, 2017). Since the  
430 harbours were no longer usable, the people left the city. Most probably fearing pirate attacks,  
431 they moved to the landward settlement of *Püsküllü Tepeler* (Pirson, 2010; Seeliger *et al.*,  
432 2014). As documented by pollen data, the natural vegetation grew back and many areas  
433 became woodland again (Shumilovskikh *et al.*, 2016). Saltworks were constructed, mostly  
434 built using spolia, about 2 km south of the city in the shallow bay. Salt was of great economic  
435 value and it was easy to harvest using a small workforce. Very shallow marine conditions and  
436 a very low energy wave climate in the bay favoured its use as a saltworks (Pirson, 2014;  
437 Seeliger *et al.*, 2014).

438

#### 439 *Elaia in the broader context of the Turkish Aegean coast*

440 Most ancient settlements in the Turkish Aegean region were situated along the coasts of  
441 enlarged marine embayments, formed during the Holocene marine transgression. Around  
442 6000 BP, when sea-level rise slowed (Lambeck, 1996; Lambeck and Purcell, 2007), rivers  
443 became prominent morphogenetic agents, governing coastal changes by sediment supply, due  
444 to their prograding deltas. These settlements – for instance, Troy, Ainos, Ephesus, and

445 Miletos – faced numerous environmental challenges, such as the siltation of their harbours or  
446 the loss of their connection to the open sea (for location see Fig. 1b).

447 Troy is one of the most famous and best-studied examples (Figs. 1b, 10a; Kraft *et al.*, 1980,  
448 2003). At the end of the Holocene marine transgression, the sea penetrated inland, about 10  
449 km south of the later location of Troy. Deltaic progradation of the Scamander and Simois  
450 River followed by floodplain aggradation led to a northward shift of the shoreline. In the early  
451 Bronze Age (circa 3300 BC) Troy, as well as the Neolithic settlement of Kumtepe, were  
452 seaboard sites – comparable to the scene around 1500 BC in Elaia (Fig. 9) – protruding into a  
453 shallow marine embayment that still reached some kilometres further south and east of the  
454 settlements. At the time of the mythical Trojan War at the end of the late Bronze Age (most  
455 probably around 1200 BC) the delta front lay beyond but close to the settlement (Kraft *et al.*,  
456 1980, 2003; Hertel, 2008; Brown, 2017). The present shoreline is situated some 4 km north of  
457 Troy and a strong longshore drift has hindered a further seaward progradation of the delta  
458 (Fig. 10a). Due to the long settlement history (3300 BC until AD 1200/1300 with  
459 interruptions, Troia I–Troia IX), the city hosted different harbour sites following the migrating  
460 shoreline. Based on a detailed summary of published work since the 1980s, Kayan (2014)  
461 suggests three possible harbour locations on the eastern slope of the Sigeion ridge (Fig. 10a).  
462 However, the southernmost possible location in the Yeniköy plain (YE in Fig. 10a) was  
463 already landlocked between 5000–3500 BP and a westward connection to the open Aegean by  
464 a canal or ditch crossing the Sigeion ridge is to be excluded in that case. Meanwhile, the  
465 silting up history of the Keşik plain (KE in Fig. 10a) is still open to discussion. While Kayan  
466 (2014) states a swamp at the time of the Trojan War, Kraft *et al.* (2003) assume a near-coastal  
467 shallow marine embayment in this area. In contrast to the Yeniköy plain, an opportunity to  
468 transport ships to the other side of the Sigeion ridge was proven for the Keşik plain. It was  
469 possible to transport ships from a protected harbour location in this area to the Aegean  
470 although the delta front had already prograded beyond this location. Finally, the northernmost  
471 area of the Kumtepe plain (KT in Fig. 10a) silted up last, most probably in late Hellenistic or  
472 early Roman Imperial times. Although Kayan (2014) does not advocate a harbour in this area,  
473 it would have been possible to land vessels at this location throughout the settlement period of  
474 Troy (Kraft *et al.*, 2003; Hertel, 2008; Kayan, 2014).

475 The ancient city of Ainos (Fig. 1b) is located close to the river mouth of the Hebros, which  
476 today debouches into the Aegean via an extensive deltaic floodplain of 180 km<sup>2</sup>, between the  
477 Greek city of Alexandroupoli and the Turkish city Enez. Postglacial sea-level rise created a  
478 marine embayment which reached as far as the modern town of İpsala, i.e., 26 km inland.

479 Later, the delta front passed the city just after Roman Imperial times and may have caused a  
480 shift in the location of the city's harbours. Today, the city is situated about 2.5 km inland,  
481 separated from the Aegean by an extensive beach-barrier system (Alpar, 2001; Anthony *et al.*,  
482 2014; Brückner *et al.*, 2015).

483 Further south, at ancient Ephesus (Fig. 1b) and its famous Artemision, sediment transported  
484 by the Küçük Menderes River led to a widespread siltation of the Küçük Menderes graben.  
485 The prograding delta caused a siltation of the harbours and the Ephesians were eventually  
486 forced to construct a "harbour channel" to maintain an access route to the sea after the delta  
487 front prograded beyond the city (e.g. Kraft *et al.*, 2007; Delile *et al.*, 2015; Ledger *et al.*,  
488 2018).

489 Finally, the palaeoenvironmental model of Küçük Menderes graben can also be transposed to  
490 the Büyük Menderes graben, circa 50 km south. As the longest waterway flowing into the  
491 Turkish Aegean, the Büyük Menderes River led to the disconnection of ancient Miletos and  
492 Priene, situated on the southern flank of the Büyük Menderes graben, from the open sea and  
493 the demise of their harbours (e.g. Brückner *et al.*, 2006, 2013; Kazancı *et al.*, 2009).

494 In contrast, Fig. 10b presents the coastal configuration of the wider Elaia region. Unlike the  
495 above-mentioned settlements, Elaia is not situated on the inner part of the Kaikos- or  
496 Zeytindağ graben. The Bozyertepe ridge separates it from the Zeytindağ graben and therefore  
497 protects it from the fluvial sediments of the Kaikos. This is supported by the absence of  
498 fluvial sediments in the cores (unit 6). The siltation of the harbours of Elaia was therefore not  
499 as strong triggered by deltaic progradation as for the above mentioned examples, but also by  
500 slope wash of terrestrial material from the nearby Yuntdağ and Bozyertepe. As studies  
501 investigating the deltaic evolution of the Kaikos are lacking at present, it is speculative to  
502 further comment on this topic. Nevertheless, remains of a Roman-age bridge, just west of the  
503 Bozyertepe, documents that the delta front had already prograded beyond this location before  
504 this date. Based on corings, the evolution of the small island (I on Fig. 10b) was dated to post-  
505 15<sup>th</sup> century AD (Körfgén, 2014), showing that the most distal extension of the delta  
506 happened recently. As a result, because the influence of a major river delta is secondary, the  
507 harbour basins of Elaia were not massively affected by siltation which is borne out by the  
508 absence of dredging. Dredging is widely attested in other Mediterranean harbours such as  
509 Naples (Delile *et al.*, 2016), Portus (Salomon *et al.*, 2012), Tyre (Marriner and Morhange,  
510 2006), Marseille (Morhange *et al.*, 2003) and Ephesus (Kraft *et al.*, 2007; Delile *et al.*, 2015).  
511 In addition, due to the short settlement period of Elaia (maximum 1000 years) – bracketed by



512 natural conditions before and after it – the closed harbour basin constitutes a valuable  
513 geocache (Shumilovskikh *et al.*, 2016).

514

## 515 **Conclusion**

516 Around 1500 BC, the marine extension in the Bay of Elaia was at its maximum. The sea  
517 protruded circa 400 m inland in the northern and western areas; thus, the Acropolis was  
518 transformed into a peninsula. Due to the adjacent Yuntdağ Mountains, the extension of the sea  
519 to the east of Elaia was far less significant than in the western part. Siltation led to a gradual  
520 regression of the shoreline, mostly due to human activities during the ensuing centuries  
521 (Shumilovskikh *et al.*, 2016).

522 During Hellenistic and Roman times, from ~300 BC onwards, three harbour areas were  
523 operational: the closed harbour, the open harbour, and the beach harbour. While the closed  
524 harbour was used for commercial and military purposes, the open harbour most likely housed  
525 the ship sheds with the battleships of the Pergamenians. The eastern city district with its beach  
526 harbour served as a place of temporary residence for foreign merchants, sailors, and soldiers  
527 (Pirson, 2010, 2014; Seeliger *et al.*, 2017; Pint *et al.*, 2015; Feuser *et al.*, 2018). The siltation  
528 of the harbours contributed to the decline of the city in late Roman times led to its eventual  
529 abandonment (after AD 500). Human activities hugely influenced landscape changes. First of  
530 all, erosional processes became prominent in the densely populated and intensively used  
531 eastern part of the Bay of Elaia while these impacts were relatively minor in the western part,  
532 far from the settled area. Pint *et al.* (2015) have already demonstrated that the siltation of the  
533 open harbour area accelerated during the settlement period of Elaia. This may have resulted  
534 from the construction of the closed harbour basin and its breakwaters while impeding the  
535 bay's counterclockwise coastal cell, creating a sediment trap east of the closed harbour  
536 directly in front of the open harbour area (Figs. 2, 9).

537 While the population of Elaia shrank during Late Antiquity, the remaining inhabitants went to  
538 great lengths to construct the saltworks, which definitely had a strong influence on the  
539 environment and the sea currents in this area. Finally, in contrast to many other ancient  
540 settlements on the Turkish Aegean coast, Elaia was not significantly affected by siltation of a  
541 major river delta. As a consequence, no indications – neither sedimentological or literary –  
542 report dredging inside Elaia's different harbours. Due to the relatively short urban period of  
543 around 1000 years Elaia has a particular potential to study human-nature relations in the  
544 Hellenistic-Roman Imperial period, and the abandonment of a late antique city and the  
545 subsequent return to natural conditions (Shumilovskikh *et al.*, 2016; Pirson, in print).

546

## 547 **Acknowledgements**

548 Financial support from the German Research Foundation is gratefully acknowledged (DFG  
549 ref. no. PI 740/1–3). Our research was part of the greater Elaia-Survey Project, headed by  
550 Felix Pirson, Director of the DAI Istanbul and excavation director of Pergamon. The Ministry  
551 of Culture and Tourism of the Republic of Turkey kindly granted the research permits. This  
552 work is a contribution to IGCP Project 639 “*Sea-Level Changes from Minutes to Millennia*”.  
553 Svenja Riedesel acknowledges financial support from an AberDoc-PhD scholarship  
554 (Aberystwyth University, UK). We acknowledge constructive comments by the editor of JQS  
555 Geoff Duller (Aberystwyth University, UK) and by Matteo Vacchi (University of Exeter,  
556 UK).

557

## 558 **References**

- 559 Ad-Hoc-AG Boden. 2005. *Bodenkundliche Kartieranleitung*. Schweizerbart: Stuttgart. (in  
560 German)
- 561 Aksu AE, Piper DJW, Konuk T. 1987. Late Quaternary tectonic and sedimentary history of  
562 outer İzmir and Çandarlı Bays, Western Turkey. *Marine Geology* **76**: 89–104.
- 563 Alpar B. 2001. Plio-Quaternary history of the Turkish coastal zone of the Enez-Evros Delta:  
564 NE Aegean Sea. *Mediterranean Marine Science* **2(2)**: 95–118.
- 565 Altunkaynak S, Yilmaz Y, 1998. The Mount Kozak magmatic complex. *Western Anatolia*  
566 *Journal of Volcanology and Geothermal Research* **85**: 211–231.
- 567 Ammerman AJ, Efstratiou N, Ntinou M *et al.* 2008. Finding the early Neolithic in Aegean  
568 Thrace: the use of cores. *Antiquity* **315**: 139–150.
- 569 Anthony EJ, Marriner N, Morhange C. 2014. Human influence and the changing  
570 geomorphology of Mediterranean deltas and coasts over the last 6000 years: from  
571 progradation to destruction phase? *Earth-Science Reviews* **139**: 336–361.
- 572 Bartz M, Klasen N, Zander A *et al.* 2015. Luminescence dating of ephemeral stream  
573 sediments around the Palaeolithic site of Ifri n'Ammar (Morocco). *Quaternary*  
574 *Geochronology* **30**: 460–465.
- 575 Bartz M, Rixhon G, Kehl M *et al.* 2017. Unravelling fluvial deposition and pedogenesis in  
576 ephemeral stream deposits in the vicinity of the prehistoric rock shelter of Ifri n'Ammar  
577 (NE Morocco) during the last 100 ka. *Catena* **152**: 115–134.
- 578 Başaran S. 2010. *Ainos (Enez)*, University İstanbul Press, İstanbul.
- 579 Benjamin J, Rovere A, Fontana A *et al.* 2017. Late Quaternary sea-level changes and early  
580 human societies in the central and eastern Mediterranean Basin: An interdisciplinary  
581 review. *Quaternary International* **449**: 29–57.

- 582 Blott SJ, Pye K. 2001. GRADISTAT: a grain size distribution and statistics package for the  
583 analysis of unconsolidated sediments. *Earth Surface Processes and Landforms* **26**: 1237–  
584 1248.
- 585 Bonaduce G, Ciampo G and Masoli M. 1975. Distribution of Ostracoda in the Adriatic Sea.  
586 *Pubblicazioni della Stazione zoologica di Napoli* **40** (Suppl.): 1–304.
- 587 Brown J. 2017. *Homeric Sites Around Troy*, Parrot Press, Canberra.
- 588 Brückner H. 1994. Das Mittelmeergebiet als Naturraum. In *Das Alte Rom*, Martin J (ed).  
589 Bertelsmann, München, 13–29.
- 590 Brückner H, Müllenhoff M, Gehrels R *et al.* 2006. From archipelago to floodplain -  
591 geographical and ecological changes in Miletus and its environs during the past six  
592 millennia (Western Anatolia, Turkey). *Zeitschrift für Geomorphologie N.F.* **142** (Suppl):  
593 63–83.
- 594 Brückner H, Urz R, Seeliger M. 2013. Geomorphological and geoarchaeological evidence for  
595 considerable landscape changes at the coasts of western Turkey during the Holocene.  
596 *Geopedology and Landscape Development Research Series* **1**: 81–104.
- 597 Brückner H, Schmidts T, Bücherl H *et al.* 2015. Die Häfen und ufernahen Befestigungen von  
598 Ainos - eine Zwischenbilanz. In *Häfen im ersten Millennium AD. Bauliche Konzepte,*  
599 *herrschaftliche und religiöse Einflüsse*, Schmidts T, Vučetić MM (eds). Verlag des  
600 Römisch-Germanischen Zentralmuseums, Mainz, 53–76.
- 601 Cartledge P. 2004. *Alexander the Great. The Hunt for a New Past*, Overlook Press, New  
602 York.
- 603 Cimerman F, Langer MR. 1991. *Mediterranean foraminifera*. Slovenska Akademija Znanosti  
604 in Umetnosti, Academia Scientiarum et Artium Slovenica, Ljubljana.
- 605 Delile H, Blichert-Toft J, Goiran JP *et al.* 2015. Demise of a harbor: A geochemical chronicle  
606 from Ephesus. *Journal of Archaeological Science* **53**: 202–213.
- 607 Delile H, Goiran J-P, Blichert-Toft J *et al.* 2016. A geochemical and sedimentological  
608 perspective of the life cycle of Neapolis harbour (Naples, southern Italy). *Quaternary*  
609 *Science Reviews* **150**: 84–97.
- 610 Evelpidou N, Karkani A, Kampolis I *et al.* 2017. Late Holocene shorelines in east Attica  
611 (Greece). *Quaternary International* **436**: 1–7.
- 612 Ernst W. 1970. *Geochemical facies analysis*, Elsevier, Amsterdam, London, New York.
- 613 Feuser S, Pirson F, Seeliger M. 2018. The Harbour Zones of Elaia – the Maritime City of  
614 Pergamum. In *Harbours as objects of interdisciplinary research – Archaeology + History*  
615 *+ Geosciences*, von Carnap-Bornheim C, Daim F, Ettl P, Warnke U (eds). Verlag des  
616 Römisch-Germanischen Zentralmuseums, Mainz, 91–103.
- 617 Flaux C, Marriner N, el-Assal M *et al.* 2017. Late Holocene erosion of the Canopic  
618 promontory (Nile Delta, Egypt). *Marine Geology* **385**: 56–67.
- 619 Folk RL, Ward WC. 1957. Brazos River bar: a study in the significance of grain size  
620 parameters. *Journal of Sedimentary Petrology* **27**: 3–26.

- 621 Frenzel P, Boomer I. 2005. The use of ostracods from marginal-marine, brackish waters as  
622 bioindicators of modern and Quaternary environmental change. *Palaeogeography,*  
623 *Palaeoclimatology, Palaeoecology* **225(1–4)**: 68–92.
- 624 Giaime M, Morhange C, Ontiveros MAC *et al.* 2017. In search of Pollentia's southern  
625 harbour: Geoarchaeological evidence from the Bay of Alcúdia (Mallorca, Spain).  
626 *Palaeogeography, Palaeoclimatology, Palaeoecology* **466**: 184–201.
- 627 Goodman BN, Reinhardt E, Dey H *et al.* 2008. Evidence for Holocene marine transgression  
628 and shoreline progradation due to barrier development in Iskele, Bay of Izmir, Turkey.  
629 *Journal of Coastal Research* **24(5)**: 1269–1280.
- 630 Goodman BN, Reinhardt EG, Dey HW *et al.* 2009. Multi-proxy geoarchaeological study  
631 redefines understanding of the paleocoastlines and ancient harbours of Liman Tepe (Iskele,  
632 Turkey). *Terra Nova* **21(2)**: 97–104.
- 633 Hadler H, Kissas K, Koster B *et al.* 2013. Multiple Late-Holocene tsunami landfall in the  
634 eastern Gulf of Corinth recorded in the palaeotsunami geoarchive at Lechaion, harbour of  
635 ancient Corinth (Peloponnese, Greece). *Zeitschrift für Geomorphologie N.F.* **57(4)**  
636 **(Suppl)**: 139–180.
- 637 Hansen E. 1971. *The Attalids of Pergamon*, Cornell University Press, Ithaca.
- 638 Hertel D. 2008. *Troia – Archäologie Geschichte Mythos*, C. H. Beck, München.
- 639 Horejs B. 2012. Çukuriçi Höyük. A Neolithic and Bronze Age Settlement in the Region of  
640 Ephesos. In *The Neolithic in Turkey. New Excavations & New Research*, Özdoğan M,  
641 Başgelen N, Kuniholm P (eds). Archaeology and Art Publications, İstanbul, 117–131.
- 642 Horejs B, Milić B, Ostmann F *et al.* 2015. The Aegean in the Early 7<sup>th</sup> Millennium BC:  
643 Maritime Networks and Colonization. *Journal of World Prehistory* **28(4)**: 289–330.
- 644 Jeckelmann C. 1996. *Genese lokaler Thermalwasservorkommen in der Region Bergama/W-*  
645 *Türkei - Hydrochemie, Gas- und Isotopenanalysen zur Korrelation tiefer*  
646 *Grundwasserzirkulation und aktiver Tektonik*. PhD-Thesis, University of Zürich,  
647 Switzerland.
- 648 Joachim F, Langer M. 2008. *The 80 most common ostracods from the Bay of Fetoveia, Elba*  
649 *Island (Mediterranean Sea)*, University Bonn Press, Bonn.
- 650 Kayan I. 1999. Holocene stratigraphy and geomorphological evolution of the Aegean coastal  
651 plains of Anatolia. *Quaternary Science Reviews* **18**: 541–548.
- 652 Kayan I. 2014. Geoarchaeological Research at Troia and its Environs. In *Troia 1987–2012:*  
653 *Grabungen und Forschungen I – Forschungsgeschichte, Methoden und Landschaft*,  
654 Pernicka E, Rose CB, Jablonka P (eds), Verlag Dr. Rudolf-Habelt, Bonn, 694–731.
- 655 Kazancı N, Dündar S, Alçiçek MC *et al.* 2009. Quaternary deposits of the Büyük Menderes  
656 Graben in western Anatolia, Turkey: Implications for river capture and the longest  
657 Holocene estuary in the Aegean Sea. *Marine Geology* **264**: 165–176.
- 658 Khan NS, Ashe E, Shaw TA *et al.* 2015. Holocene relative sea-level changes from near-,  
659 intermediate-, and far-field locations. *Current Climate Change Reports* **1(4)**: 247–262.

- 660 Körfigen K. 2014. *Die Analyse des Bohrkerns ELA 84 – Ein Beitrag zur sedimentologischen*  
661 *Entwicklung der Bucht von Elaia, Westtürkei*. Bachelor's-Thesis, University of Cologne,  
662 Germany.
- 663 Kraft JC, Aschenbrenner SE, Rapp G Jr. 1977. Paleogeographic reconstructions of coastal  
664 Aegean archaeological sites. *Science* **195**: 941–947.
- 665 Kraft JC, Kayan I, Erol O. 1980. Geomorphic reconstructions in the environs of ancient Troy.  
666 *Science* **209**: 776–782.
- 667 Kraft JC, Rapp G, Szemler GJ *et al.* 1987. The pass at Thermopylae, Greece. *Journal of Field*  
668 *Archaeology* **14**: 181–198.
- 669 Kraft JC, Kayan I, Luce JV. 2003. Harbor areas at ancient Troy: sedimentology and  
670 geomorphology complement Homer's Iliad. *Geology* **31(2)**: 163–166.
- 671 Kraft JC, Brückner H, Kayan I *et al.* 2007. The geographies of ancient Ephesus and the  
672 Artemision in Anatolia. *Geoarchaeology* **22**: 121–149.
- 673 Lambeck K. 1996. Sea-level change and shore-line evolution in Aegean Greece since Upper  
674 Palaeolithic time. *Antiquity* **70**: 588–611.
- 675 Lambeck K, Purcell A. 2007. Palaeogeographic reconstructions of the Aegean for the past  
676 20,000 years: Was Atlantis on Athens doorstep? In *The Atlantis Hypothesis: Searching for*  
677 *a Lost Land*, Papamarinopoulos SP (ed). Heliotos Publications, Santorini, 241–257.
- 678 Ledger ML, Stock F, Schwaiger H *et al.* 2018. Intestinal parasites from public and private  
679 latrines and the harbour canal in Roman Period Ephesus, Turkey (1st c. BCE to 6th c. CE).  
680 *Journal of Archaeological Science: Reports* **21**: 289–297.
- 681 Lubos C, Dreibrodt S, Bahr A. 2016. Analysing spatio-temporal patterns of archaeological  
682 soils and sediments by comparing pXRF and different ICP-OES extraction methods.  
683 *Journal of Archaeological Science: Reports* **9**: 44–53.
- 684 Marriner N, Morhange C. 2006. Geoarchaeological evidence for dredging in Tyre's ancient  
685 harbour, Levant. *Quaternary Research* **65**: 164–171.
- 686 Marriner N, Morhange C, Kaniewski D *et al.* 2014. Ancient harbour infrastructure in the  
687 Levant: tracking the birth and rise of new forms of anthropogenic pressure. *Scientific*  
688 *Reports* **4**: 5554.
- 689 Meriç E, Avşar N, Bergin F. 2004. Benthic foraminifera of eastern Aegean Sea (Turkey);  
690 systematics and autecology. *Turkish Marine Research Foundation* **18**: 1–306.
- 691 Morhange C, Giaime M, Marriner N *et al.* 2016. Geoarchaeological evolution of Tel Akko's  
692 ancient harbour (Israel). *Journal of Archaeological Science: Reports* **7**: 71–81.
- 693 Morhange C, Blanc F, Bourcier M *et al.* 2003. Bio-sedimentology of the late Holocene  
694 deposits of the ancient harbour of Marseilles (Southern France, Mediterranean Sea). *The*  
695 *Holocene* **13**: 593–604.
- 696 Murray JW, 2006. *Ecology and Applications of Benthic Foraminifera*, Cambridge University  
697 Press, New York.

- 698 Murray-Wallace CV, Woodroffe CD. 2014. *Quaternary Sea-Level Changes: A Global*  
699 *Perspective*, Cambridge University Press, Cambridge.
- 700 Özbek O. 2010. Hamaylitarla reconsidered: A Neolithic site and its environmental setting in  
701 southern Thrace. *Anatolia Antiqua* **18(1)**: 1–21.
- 702 Pennington BT, Sturt F, Wilson P *et al.* 2017. The fluvial evolution of the Holocene Nile  
703 Delta. *Quaternary Science Reviews* **170**: 212–231.
- 704 Pint A, Seeliger M, Frenzel P *et al.* 2015. The environs of Elaia's ancient open harbour - a  
705 reconstruction based on microfaunal evidence. *Journal of Archaeological Science* **54**: 340–  
706 355.
- 707 Pirson F. 2004. Elaia, der maritime Satellit Pergamons. *Istanbuler Mitteilungen* **54**: 197–213.
- 708 Pirson F. 2007. Elaia. *Archäologischer Anzeiger* **2007(2)**: 47–58.
- 709 Pirson F. 2008. Das Territorium der hellenistischen Residenzstadt Pergamon –  
710 Herrschaftlicher Anspruch als raumbezogene Strategie. In *Räume der Stadt - Von der*  
711 *Antike bis heute*, Jöchner C (ed). Reimer: Berlin; 27–50.
- 712 Pirson F. 2010. Survey. *Archäologischer Anzeiger* **2010(2)**: 195–201.
- 713 Pirson F. 2011. Elaia. *Archäologischer Anzeiger* **2011(2)**: 166–174.
- 714 Pirson F. 2014. Elaia, der (maritime) Satellit Pergamons. In *Harbour Cities in the Eastern*  
715 *Mediterranean from Antiquity to the Byzantine Period*, Ladstätter S, Pirson F, Schmidts T  
716 (eds), Ege Yayinlari, İstanbul, 339–356.
- 717 Pirson F. (in print). Nature, Religion, and Urban Aesthetics in Ancient Pergamon and its  
718 Micro-region. Some Thoughts on the Potential of an 'Ecological Turn' for Classical  
719 Archaeology (and beyond). In *Ecologies, Aesthetics, and Histories of Art*, Baader H, Ray  
720 S, Wolf G, (eds.), de Gruyter, Berlin. Pirson F. Scholl A. 2015. *Pergamon. A Hellenistic*  
721 *Capital in Anatolia*, Ege Yayinlari, İstanbul.
- 722 Radt W. 2016. *Pergamon – Geschichte und Bauten einer antiken Metropole*. Primus Verlag:  
723 Darmstadt.
- 724 Reimer PJ, Bard E, Bayliss A *et al.* 2013. IntCal13 and MARINE13 radiocarbon age  
725 calibration curves 0-50000 years calBP. *Radiocarbon* **55(4)**: 1869–1887.
- 726 Salomon F, Delile H, Goiran J-P *et al.* 2012. The Canale di Comunicazione Traverso in  
727 Portus: The Roman sea harbour under river influence (Tiber delta, Italy). *Géomorphologie*  
728 **1**: 75–90.
- 729 Seeliger M, Bartz M, Erkul E *et al.* 2013. Taken from the sea, reclaimed by the sea: The fate  
730 of the closed harbour of Elaia, the maritime satellite city of Pergamum (Turkey).  
731 *Quaternary International* **312**: 70–83.
- 732 Seeliger M, Brill D, Feuser S *et al.* 2014. The purpose and age of underwater walls in the Bay  
733 of Elaia of western Turkey: A multidisciplinary approach. *Gearchaeology* **29**: 138–155.
- 734 Seeliger M, Pint A, Frenzel P *et al.* 2017. Foraminifera as markers of Holocene sea-level  
735 fluctuations and water depths of ancient harbours – A case study from the Bay of Elaia (W  
736 Turkey). *Palaeogeography, Palaeoclimatology, Palaeoecology* **482**: 17–29.

- 737 Seeliger M, Pint A, Frenzel P *et al.* 2018. Using a Multi-Proxy Approach to Detect and Date a  
738 Buried part of the Hellenistic City Wall of Ainos (NW Turkey). *Geosciences* **8(10)**, 357.
- 739 Shumilovskikh LS, Seeliger M, Feuser S *et al.* 2016. The harbour of Elaia: A palynological  
740 archive for human/environmental interactions during the last 7500 years. *Quaternary*  
741 *Science Reviews* **149**: 167–187.
- 742 Siani G, Paterne M, Arnold M *et al.* 2000. Radiocarbon reservoir ages in the Mediterranean  
743 Sea and Black Sea. *Radiocarbon* **42**: 271–280.
- 744 Stock F, Ehlers L, Horejs B *et al.* 2015. Neolithic settlement sites in Western Turkey -  
745 palaeogeographic studies at Çukuriçi Höyük and Arvalya Höyük. *Journal of*  
746 *Archaeological Science: Reports* **4**: 565–577.
- 747 Strabo. 2005. *Geographica*. Translation and comments by Albert Forbiger, Marix Verlag,  
748 Wiesbaden.
- 749 Vacchi M, Rovere A, Chatzipetros A *et al.* 2014. An updated database of Holocene relative  
750 sea level changes in NE Aegean Sea. *Quaternary International* **328-329**: 301–310.
- 751 Vacchi M, Marriner N, Morhange C *et al.* 2016a. Multiproxy assessment of Holocene relative  
752 sea-level changes in the western Mediterranean: sea-level variability and improvements in  
753 the definition of the isostatic signal. *Earth-Science Reviews* **155**: 172–197.
- 754 Vacchi M, De Falco G, Simeone S *et al.* 2016b. Biogeomorphology of the Mediterranean  
755 *Posidonia oceanica* seagrass meadows. *Earth Surface Processes and Landforms* **42**: 42–  
756 54.
- 757 Vita-Finzi C. 1969. Late Quaternary continental deposits of central and western Turkey. *Man*  
758 *New Series* **4(4)**: 605–619.
- 759 Vött A, Bareth G, Brückner H *et al.* 2011. Olympia's harbour site Pheia (Elis, Western  
760 Peloponnese, Greece) destroyed by tsunami impact. *Die Erde* **142(3)**: 259–288.
- 761 Yoo J, Rohli RV. 2016. Global distribution of Köppen–Geiger climate types during the Last  
762 Glacial Maximum, Mid-Holocene, and present. *Palaeogeography, Palaeoclimatology,*  
763 *Palaeoecology* **446**: 326–337.
- 764 Zimmermann M. 2011. *Pergamon: Geschichte, Kultur, Archäologie*, C.H. Beck, München.

## 765 **Caption of Figures and Tables**

766 **Figure 1.** The study area on the Aegean coast of Turkey. (a) Structural map and surrounding mountain  
767 ranges. Bergama and Zeytindağ grabens are marked in yellow. The study area of Elaia (Fig. 2a) is  
768 denoted in pale red. Source: Altunkaynak and Yilmaz (1998), substantially modified, with locations  
769 mentioned in the text. Insert: (b) General map of the Turkish Aegean coast with the position of the  
770 study area (Fig. 1a) and further ancient settlements mentioned in this paper. Source: Radt (2016),  
771 substantially modified. (c) Timeline of the historical periods, linked with the period of Elaia's prime  
772 (based on: Pirson and Scholl, 2015; Radt, 2016).

773 **Figure 2.** Locations of selected vibracores taken in the Bay of Elaia. (a) Locations of coring transects  
774 A–A', B–B', D–D', E–E' and F–F', "C" (coring Ela 58), and of the elevation profile XYZ shown in  
775 Fig. 2c. (b) Panoramic view of the study area (UAV image; taken on 01 September 2015 by A. Bolten)  
776 with the location of the harbour areas. (c) Elevation profile XYZ (based on Google Earth Pro; 21 July  
777 2018). The enhanced relief energy of the eastern part in contrast to the western area of the Bay of Elaia  
778 is clearly evident.

779 **Figure 3.** Sediment core Ela 57 with geochemical and sedimentological parameters (a, b, c). (d)  
780 Interpretation of sedimentary units and dating results.

781 **Figure 4.** Sedimentary units of core Ela 57, based on microfauna. Relative abundance of ostracods and  
782 foraminifers is given semi-quantitatively.

783 **Figure 5.** Sediment core Ela 12 with geochemical and sedimentological parameters (a, b, c). (d)  
784 Interpretation of sedimentary units and dating result.

785 **Figure 6.** Sedimentary units of core Ela 12, based on microfauna. Relative abundance of ostracods and  
786 foraminifers is given semi-quantitatively.

787 **Figure 7.** Microfaunal, granulometric, and geochemical characteristics of the sedimentary units of the  
788 corings in the Bay of Elaia. Because these characteristics are dependant on regional factors (bedrock,  
789 weathering conditions etc.) care should be exercised before transposing these data to other study areas.

790 **Figure 8.** Synopsis of the coring transects (a) A–A', (b) B–B', (d) D–D', (e) E–E', and (f) F–F', as  
791 well as (c) (Ela 58); (g) legend; (h) locations of corings and transects.

792 **Figure 9.** Coastline changes in the Bay of Elaia in time slices: 1500 BC, 300 BC and AD 500. The  
793 scenarios are based on the results of this paper.

794 **Figure 10.** Comparison of the palaeoenvironmental evolution of Troy and Elaia. (a) The area of  
795 ancient Troy in Roman times. It clearly shows the influence of the Simois and Scamander Rivers on  
796 the surroundings of Troy, especially with regards to the coastline scenarios for 3300 BC (Late  
797 Neolithic/Early Bronze Age), 1300 BC (Iliad/Trojan War) and Roman times (based on Kraft *et al.*,  
798 2003; abbreviations: KT=Kum-Tepe plain, KE=Keşik plain, YE=Yeniköy plain). (b) Present coastline  
799 configuration of the Bay of Elaia and the southernmost part of the Kaikos River added by assumed  
800 former coastlines of the Kaikos Delta. It becomes evident that the prograding delta of the Kaikos River  
801 did not influence the Bay of Elaia due to the shielding effect of the Bozyertepe ridge (personal  
802 compilation based on a QuickBird 2 satellite image, acquired: 2 April 2006).

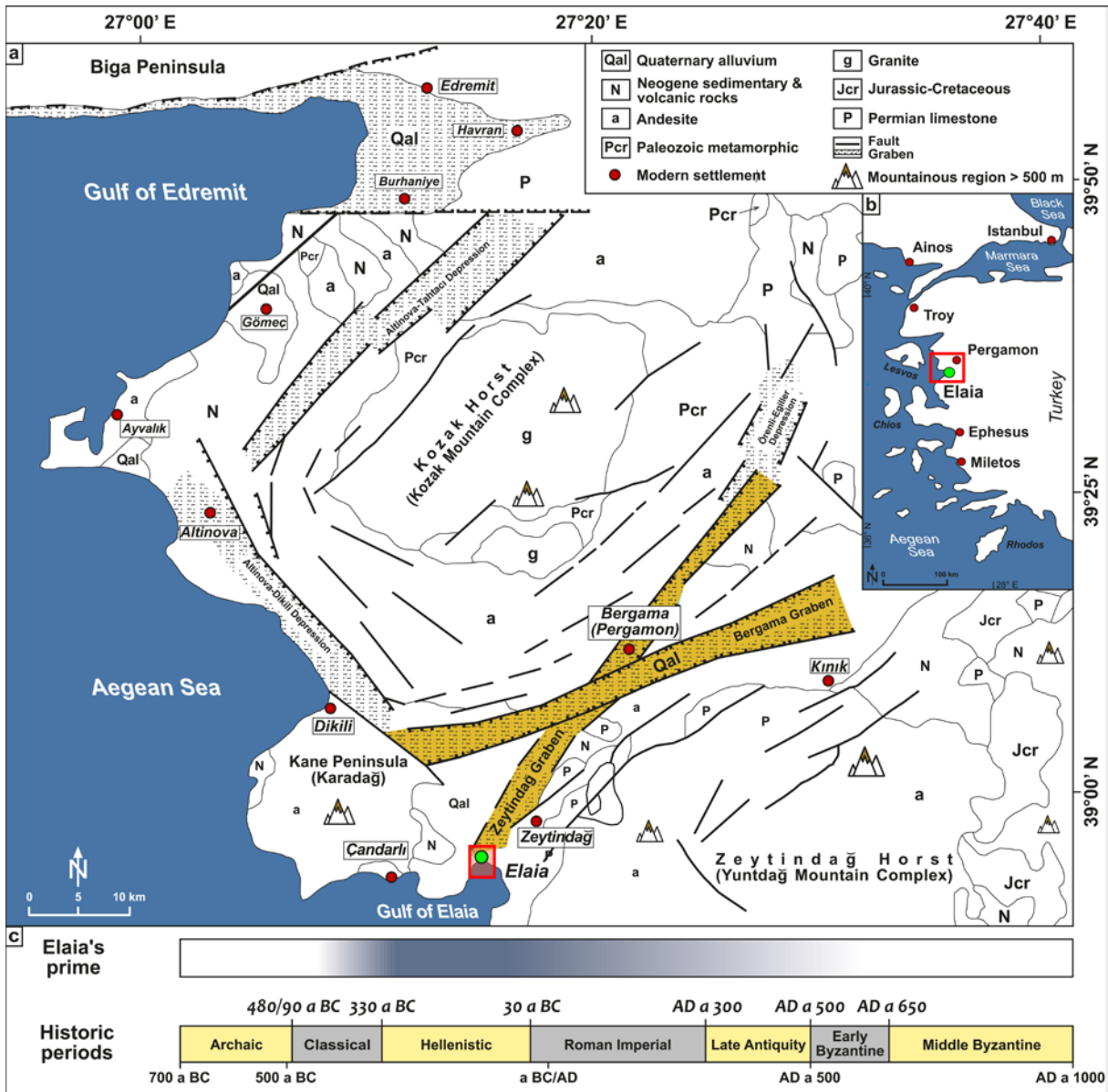
803

804 **Table 1:** Radiocarbon data sheet. <sup>14</sup>C-AMS dating was carried out at the Centre for Applied Isotope  
805 Studies (CAIS) of the University of Georgia in Athens, USA (lab code: UGAMS) and the <sup>14</sup>Chrono  
806 Centre for Climate, the Environment, and Chronology, Queen's University Belfast, UK (lab code:  
807 UBA). All ages were calibrated with the IntCal13 or MARINE13 calibration curves depending on the  
808 samples  $\delta^{13}\text{C}$  using the recent Calib 7.1 software (Reimer *et al.*, 2013). A marine reservoir effect of



809 390±85 years and a  $\Delta R$  of 35±70 years (Siani *et al.*, 2000) was applied. The calibrated ages are  
810 presented in calendar years BC/AD and years BP with  $2\sigma$  confidence interval.

811

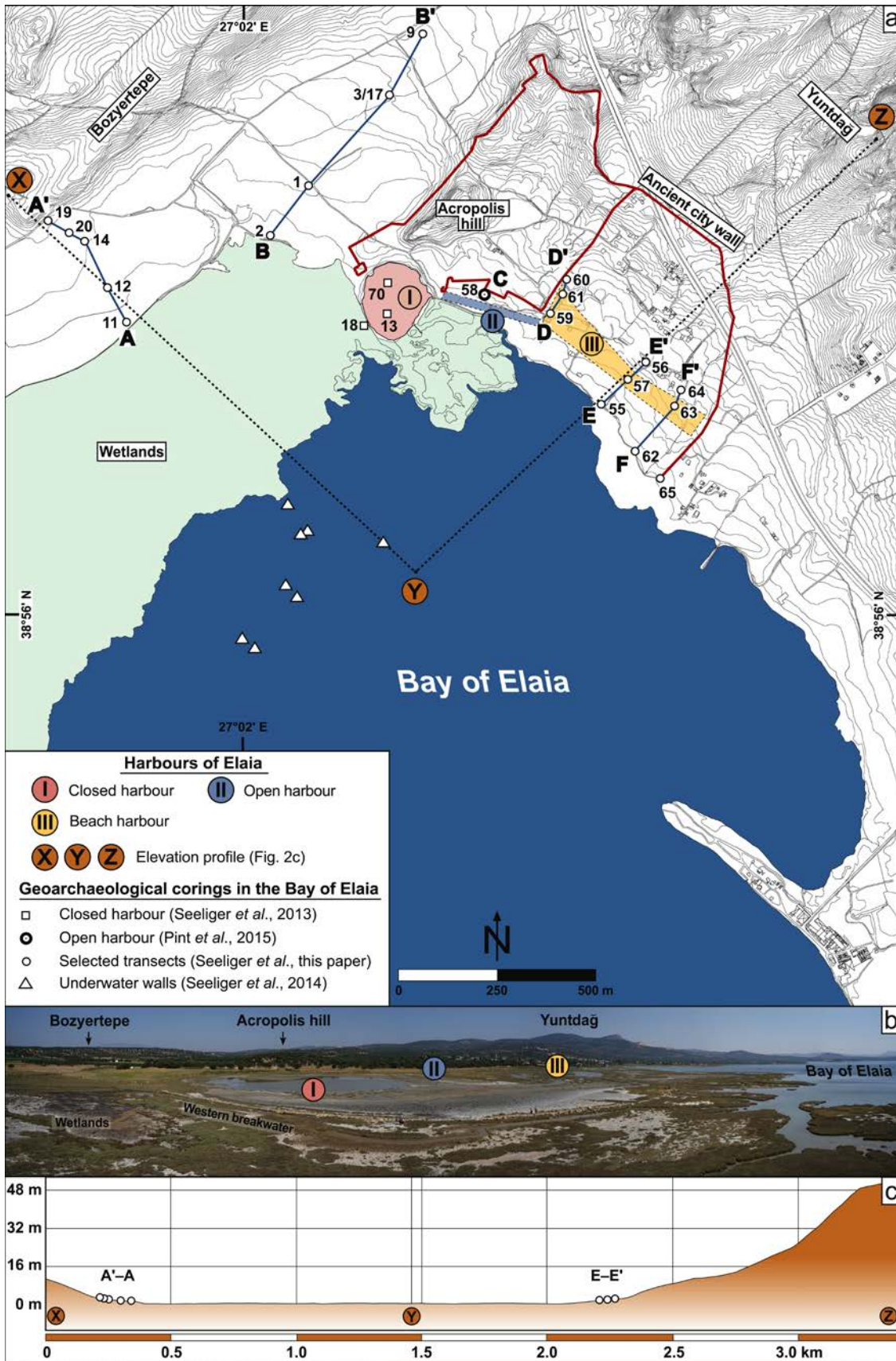


812

813 Fig. 1.

814

815



816

817

818

**Ela 57 - Central coring of E-E'**  
(27.046354° E; 38.940715° N)

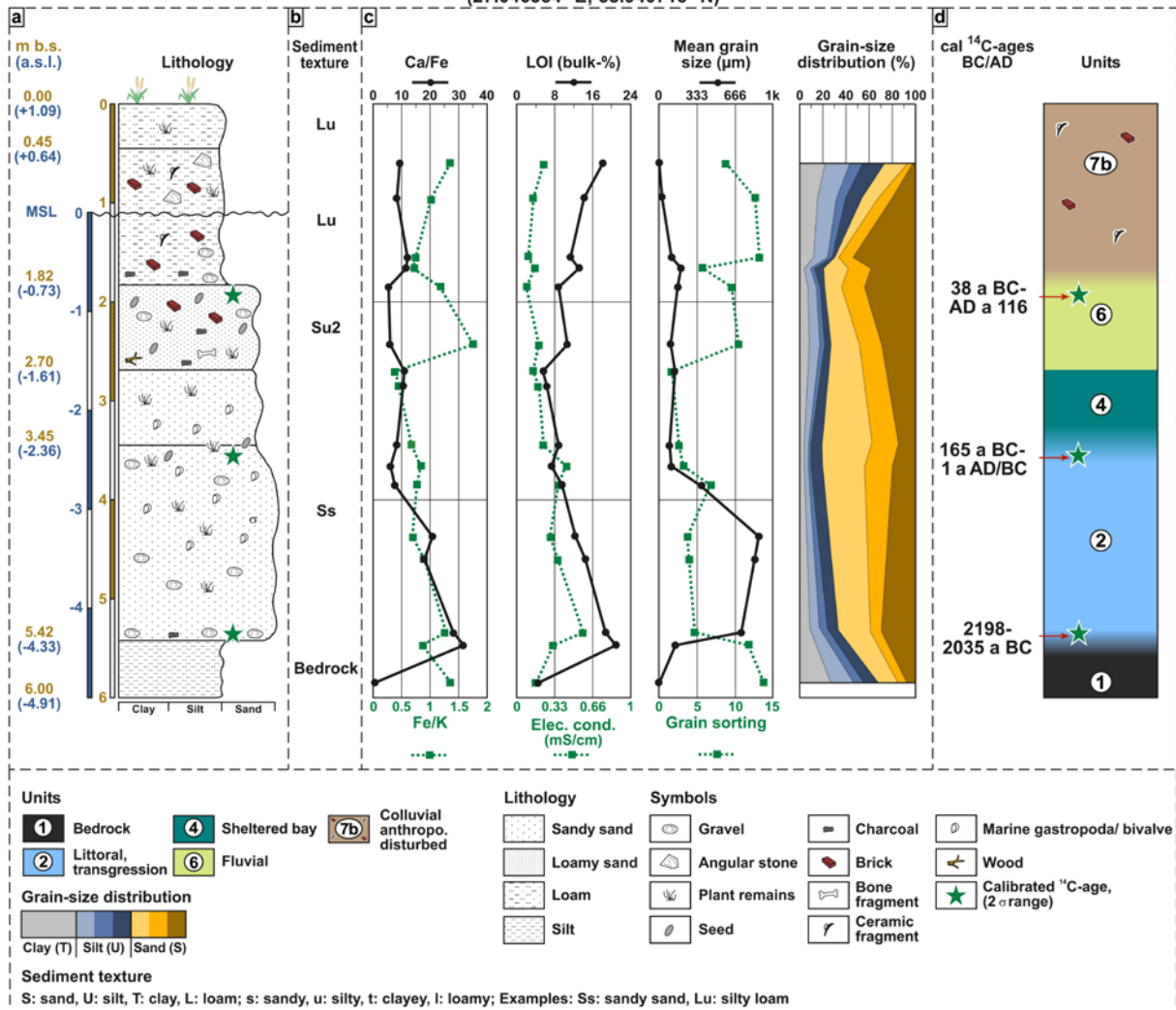


**Fig. 3.**

819  
820  
821  
822  
823

824  
825  
826  
827

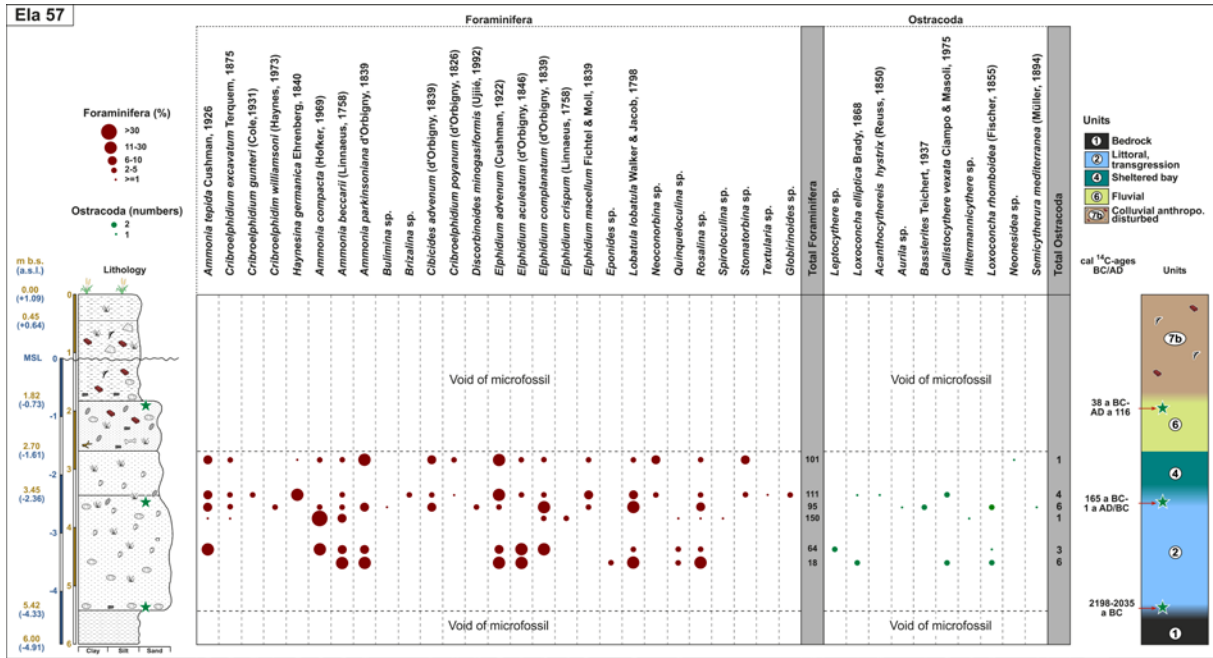
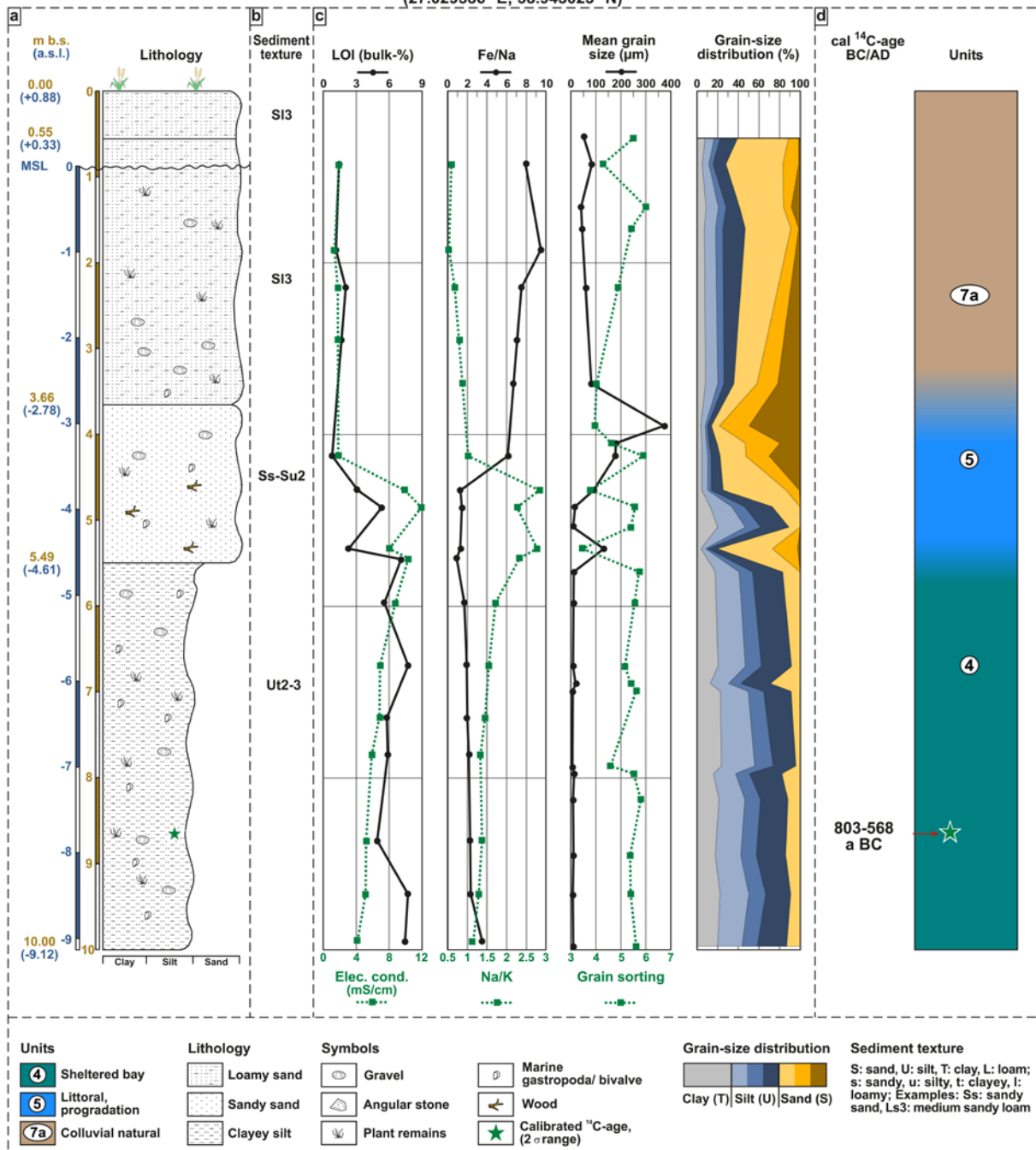


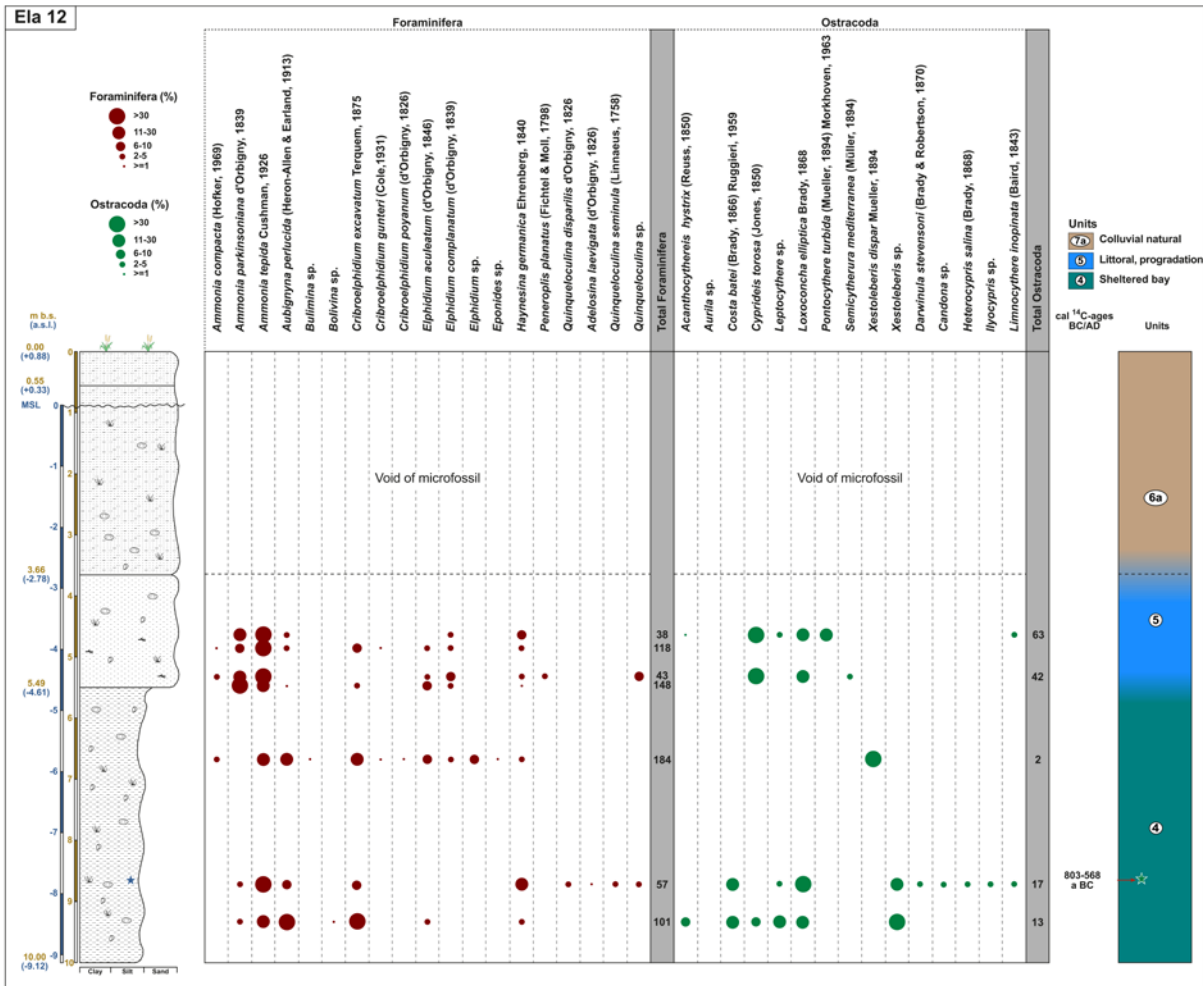
Fig. 4.

Ela 12 - Central coring of A-A'  
(27.029586° E; 38.943023° N)



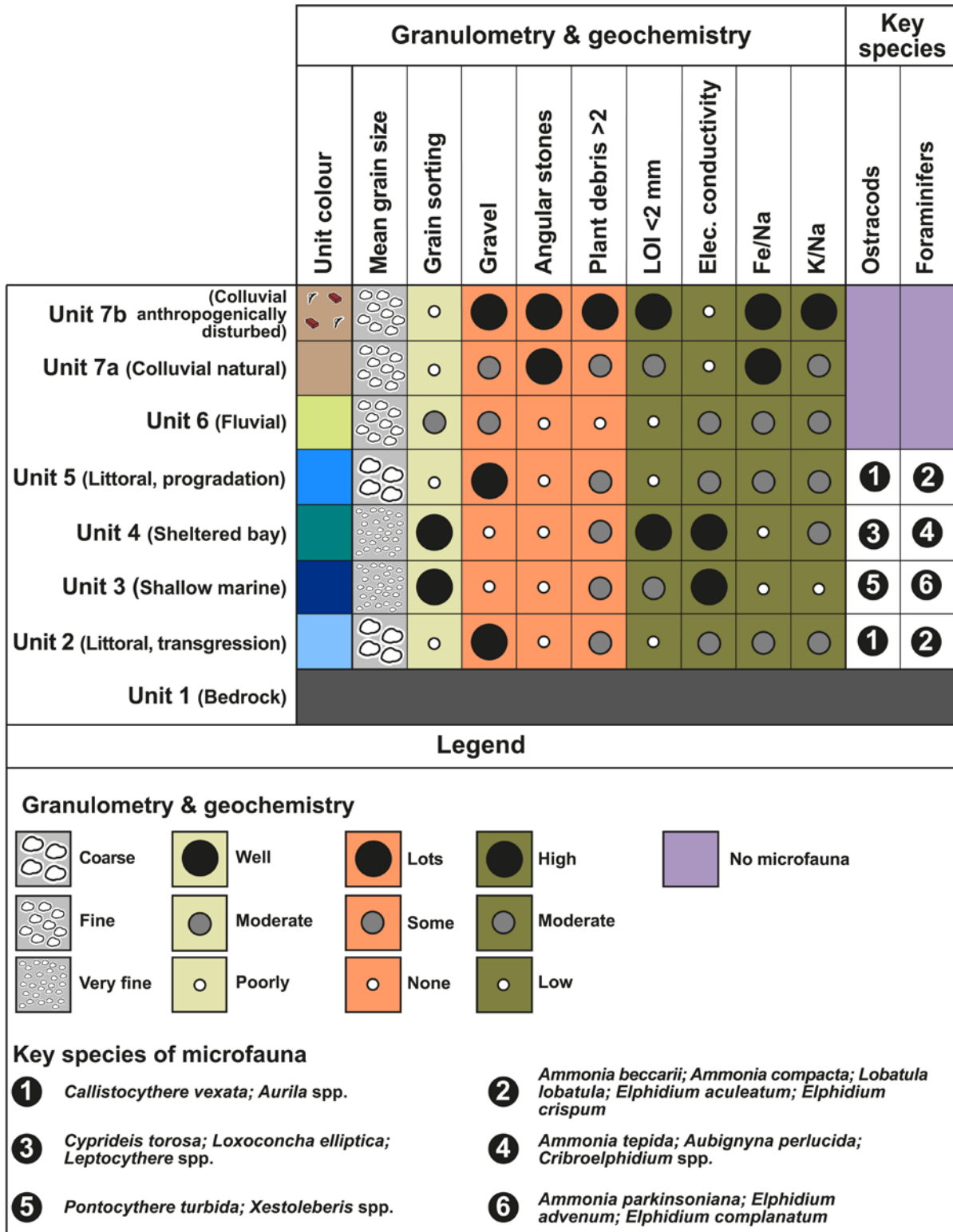
828  
829  
830

Fig. 5.



831  
832  
833  
834

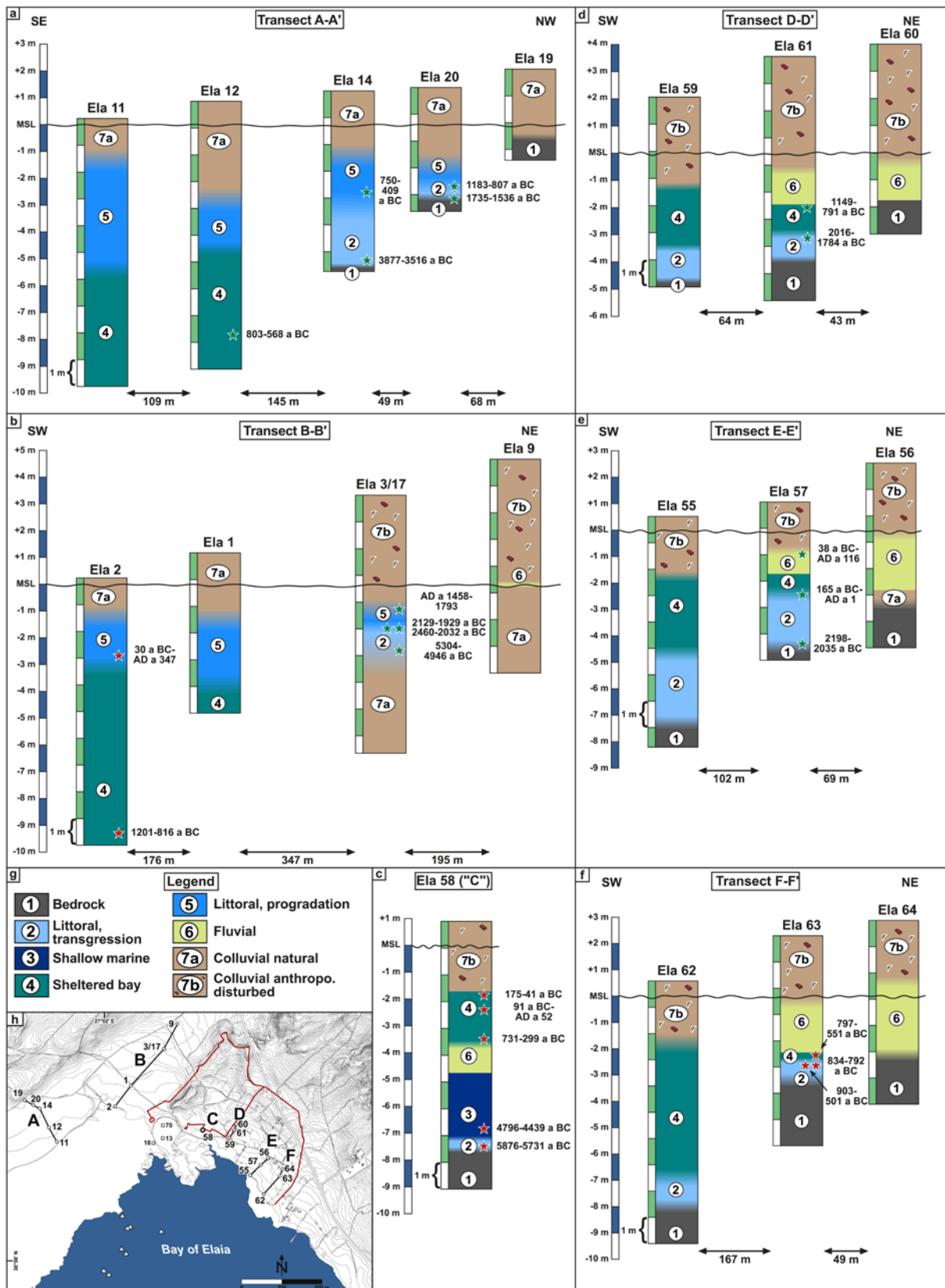
**Fig. 6.**



835  
836  
837

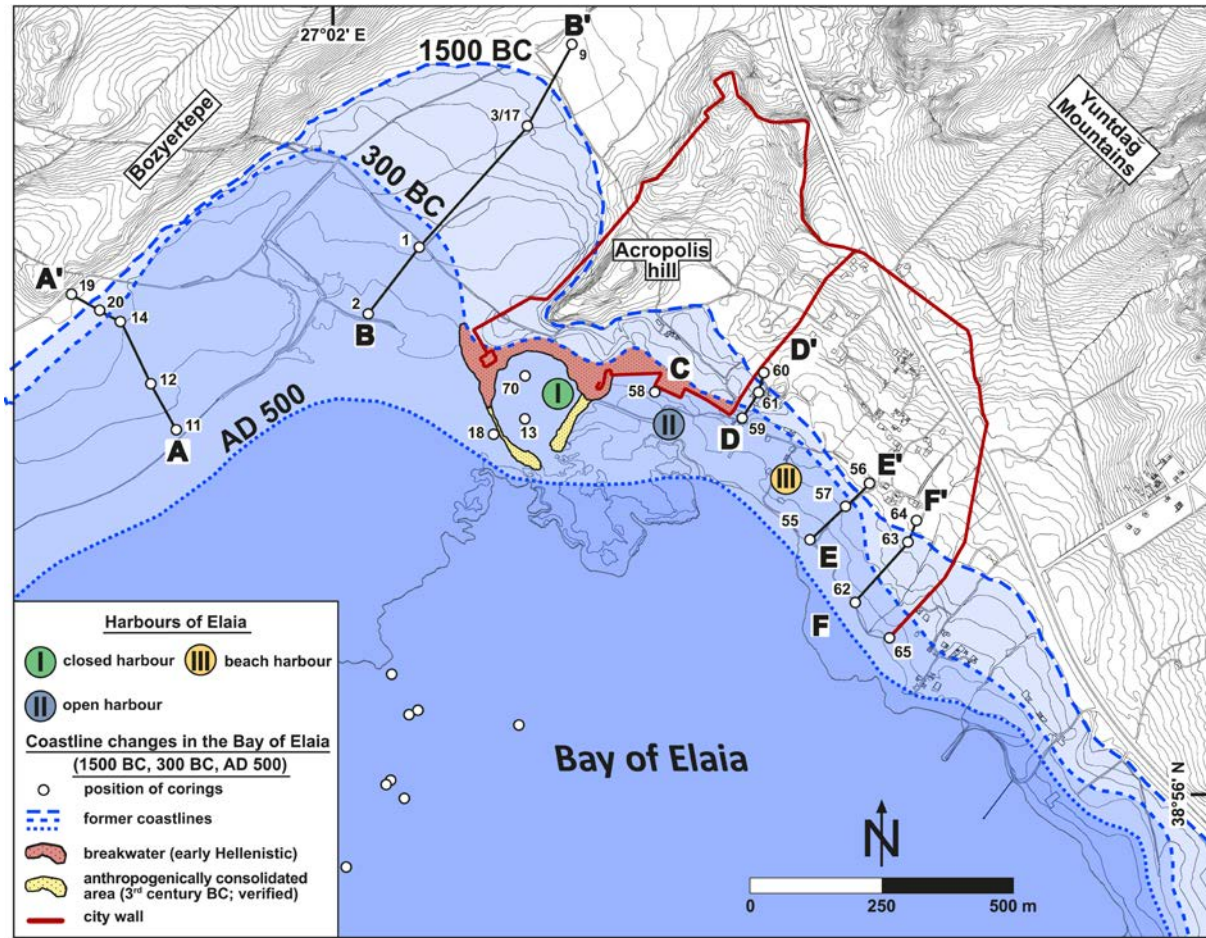
Fig. 7.





838  
839  
840  
841

Fig. 8.



842  
843 **Fig. 9.**  
844  
845

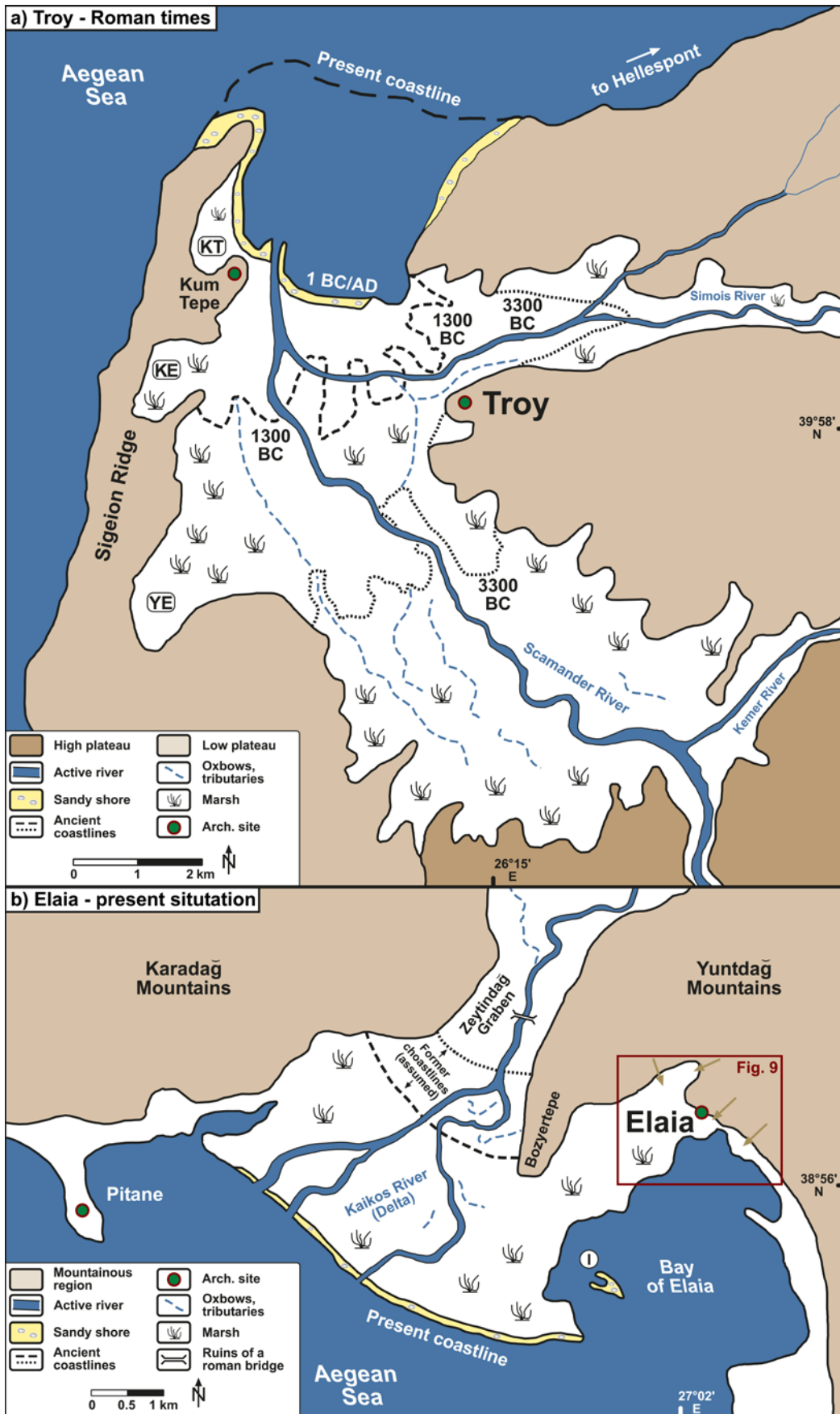


Fig. 10.

846  
847  
848